CHARACTERIZATION OF MANGANESE OXIDE COATED POROUS CARBON
AEROGEL TO ISOLATE THE EFFECTS OF ELECTRO-LESS DEPOSITION TIME, LI$^+$ -
ION EXCHANGE, AND HEAT TREATMENT ON ION SELECTIVITY AND SPECIFIC
CAPACITANCE

BY

MEKHAKHEM S. KHEPERU

THESIS

Submitted in partial fulfillment of the requirements
for the degree of Master's of Science in Environmental Engineering in Civil Engineering
in the Graduate College of the
University of Illinois at Urbana-Champaign, 2019

Urbana, Illinois

Adviser:

Assistant Professor Roland D. Cusick

Abstract

Motivated by the growing crisis of global water scarcity, this study focuses on an up and coming desalination technique. Capacitive deionization (CDI) is a novel method based on the general concept of ion electro-sorption, with two electrodes acting as capacitors [1]. When polarized in charge/discharge cycles, these cells will remove foreign ions out of brackish water and subsequently expel them into a waste stream. Recently, it has been discovered that when redox-active materials are employed, charge transfer reactions will increase the cell's ion storage capacity in proportion with mass normalized energy storage [2].

In this study, the performance of porous carbon aerogel electrodes, in terms of energy storage capacity and ion selectivity, is evaluated by varying fabrication techniques - altering electro-less deposition time of amorphous MnO_2, heat treatment for the purposes of phase transition, and Li^+- ion exchange. Additionally, we vary the electrolytic solution $(NaCl, KCl, CaCl_2, LiCl)$ in order to study the cathode's faradaic ion-uptake mechanism and the factors influencing it. Resulting nitrogen adsorption tests on the 15-minute electro-less deposition timed MnO_2- coated aerogel electrodes show low surface area per mass (170 m^2 g^{-1}), but high MnO_2 content (14.64% as compared to literature values for the same duration) implying an increased deposition rate [3]. When the pretreated carbon aerogel electrodes of varying electro-less deposition times are characterized using a three-electrode set up, resulting cyclic voltammograms in the voltage window -0.2 to 0.8 V show no relationship between electrode pretreatment and neither capacitance nor ion-uptake. Because specific capacitances are approximately the same at low and high electro-less deposition times, the optimized duration should last for 15 minutes instead of 240 minutes. Future work involves the optimization of

operation parameters such as flow rate and current density once the optimized aerogel electrodes can be incorporated into a desalination cell.

Additional work was done as educational outreach, for the purpose of investigating the most efficient methods to communicate scientific concepts to middle school students. In light of recent water contamination scandals, the students were taught methods used by engineers and average citizens to clean water containing common contaminants. Two separate student groups were chosen, one in Chicago, Illinois and one in Urbana, Illinois. These groups varied mainly in educational background and neighborhood environment. Either group was presented with a task of using two different types of filters (a granular filter and sand filter) to 'clean' contaminated water. This involved a presentation on the overview of water filtration and the engineered water cycle. Subsequently, both groups performed a hands-on activity that involved the assembly and testing of water filtration devices. Observations from presentation to the first group of students helped to better plan the second group's demo session - changes in the lesson plan included making the presentation shorter, more closely walking the students through the assembly and testing procedures, and reduction in the amount of written quizzes taken. Pre and post quizzes show the increase in knowledge of engineering, policies in the field, the engineered water cycle, and confidence in personal ability in the field of science.

I dedicate this work to my family, who have unconditionally supported my aspirations.

Acknowledgements

My thanks to Professor Roland Cusick, who has shown immense patience and understanding in my journey through graduate school. Also, I would like to thank Damon Williams, who has provided me professional and financial support throughout this process. Additionally, I would like to let Dr. Steven Hand know that I appreciated his guidance while I learned about this subject and academia in general.

Table of Contents

CHAPTER 1: INTRODUCTION

With increasing global population and environmental pollution, water scarcity is becoming a global issue. According to the United Nations, there are expected to be 2 - 7 billion people living with water stress in 2050, with water withdrawals increasing by 55%. As freshwater only makes up less than 3% of the global supply, the water treatment industry is becoming increasingly reliant on desalination and brackish water supplies [4]. With an expanding world and a shrinking water supply, humanity must learn to optimize and innovate water capture and treatment processes.

Saline water, such as sea and brackish water, must go through a process of desalting in order to be useful for most industrial and residential purposes. There are many different techniques to desalination. Currently, reverse osmosis (RO) is considered state-of-the-art – a pressure-driven membrane technology that involves applying osmotic pressure to a semi-permeable membrane separating a saline water stock from a pure water stock, rendering the diffusion and deionization of saline water energetically favorable. Even though RO is the most efficient in the field currently, the energy costs required are several times higher than the theoretical minimum. It is an extremely inefficient and energy intensive process [5] [6] [7].

Capacitive deionization (CDI) is an alternative desalination technique. By employing energy recovery and optimizing performance parameters, within brackish-level salinities, capacitive deionization has the potential to be a less energy intensive desalination method than any of the other techniques [1].

The general set up of a CDI cell consists of an anode electrically connected to a cathode, separated by a channel of saline water. The anode and the cathode are composed of symmetric electric double layer capacitors. Upon charging of the cell, these electrodes are polarized, allowing the charged ions in the saline water to be stored in the electrical double layers of the porous carbon (Figure 1A). Once the original batch is deionized, it is replaced with a high concentrate brine solution, which is meant to receive any purged ions when the voltage is reversed or removed (Figure 1B) [8] [9].
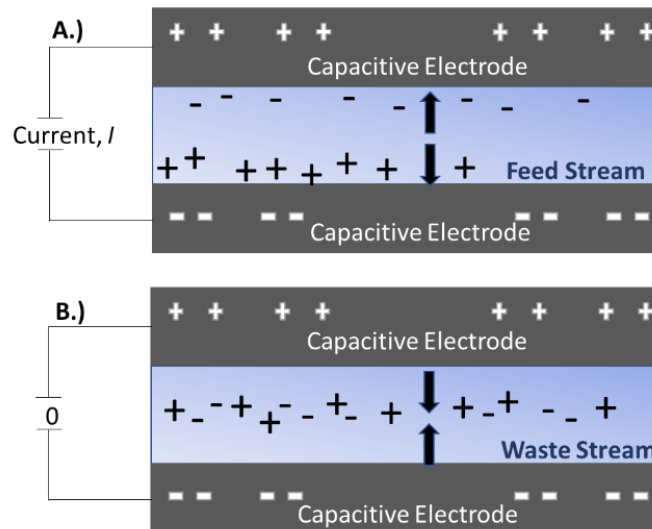

Figure 1. Diagram of conventional CDI cell. A) Adsorption. The stronger the polarization, the more ions are removed from the saline solution [24]. B) Desorption. The waste stream is a concentrated brine solution.

A common metric of potential performance is capacitance, the ability of the electrode capacitors to store ions. Significant progress has been made in recent years to increase the electrode's capacitance and thus the cell's ability to desalt feed solutions. More recently, hybrid desalination cells have coupled battery material cathodes with 3D porous carbon network

anodes. This allows for capacitive as well as faradaic ion storage, increasing the overall specific capacitance of the unit.

The stable, structurally diverse battery material sodium manganese oxide has many applications, including use in sodium ion batteries, fuel cells, and in electric grid design. It has also been employed in various atomic arrangements and phases of crystallinity as electrode material in hybrid capacitive deionization (HDCI) cells.

There are countless techniques to fabricating manganese oxide. One technique, electro-less deposition, has been shown to deposit varying amounts of amorphous, conformal manganese oxide on a porous activated carbon support depending on duration.

The objective of this work is the characterization of a composite activated carbon/transition metal oxide electrode (MnO_2 - coated carbon aerogel) through studying several fabrication procedures and their effects on electrochemical properties. Electro-less deposition duration, Li^+- ion exchange deposition, and heat treatment were experimentally altered variables of electrode fabrication. Then the resulting cyclic voltammograms profiles can be compared and analyzed for patterns concerning ion selectivity and specific capacitance.

CHAPTER 2: LITERATURE REVIEW

2.1 Water Scarcity

A concerning issue in today's world is the international water crisis. With climate change and an increasing population, water scarcity is becoming a global reality. The World Economic Forum ranks this growing scarcity as the largest threat facing the planet - potentially affecting the state of international sanitation, poverty, ecosystems and more [10]. The population facing water scarcity has increased from 14% of the global population in the 1900s to 58% in the 2000s. As of 2016, 67% of the global population (4 billion people) face severe water scarcity at least one month of the year [11]. This topic has been covered in detail by many authors, and predictions show that the resources we have will not be enough to sustain the population over the next century unless changes are made to our use and reuse of natural resources [12] [10] [13].

Around 98% of the water on earth is either sea or brackish water. Seawater can be defined as water with around 35,000 ppm of total dissolved solids (TDS). Brackish water, which is mainly held in groundwater aquifers, has a lower salinity of around 4000 ppm [14]. The purification of salt water (both brackish and seawater) is becoming increasingly crucial to the survival of humanity. There are many techniques to desalinate water, including reverse osmosis (RO), electrodialysis, and thermal separations. Regardless of the process used, a minimum energy of 1.6 kWh m^{-3} is required to desalt seawater, with 0.17 kWh m^{-3} needed for brackish water (for a recovery ratio of 0.5) [1] [15]. Reverse osmosis, a pressure-driven membrane system, is currently state-of-the-art and the fastest growing method of desalination. Still, RO involves significant energy costs, using around 2.9 - 3.7 kWh per m^3 of seawater treated, or 1.5

4

to 2.5 kWh per m^3 of brackish water. [1] [16]. This is several times the theoretical minimum to separate ions from pure water, and this energy cost is greater still with larger sized plants [17] [5] [6]. Needless to say, there is room for improvement in the energy consumption of desalination.

2.2 Introduction to CDI

Capacitive deionization (CDI) is an alternative desalination technique. It relies on the charging and discharging of a pair of electrodes, an anode and a cathode, separated by a channel. First, a saline feed stream flows through this channel and the cell is supplied with electrical energy (either constant current or constant voltage). When fully charged, the electrodes polarize and the system acts as an ideal capacitor. At this point, the charged ions in the saline solution attract to the oppositely charged electrodes, in a process called ion electro sorption. This is the adsorption step, as the ions are all stored on the surface or in lattice sites on the electrodes. The feed stream is purified, as it is now free of charged ions. Next, the purified stream is flushed out and replaced with a brine stream. This acts as a waste stream for the previously adsorbed ions once the cell is discharged by either shorting the circuit or reversing the voltage or current. If the cell is discharged under controlled conditions, the stored energy can be recovered [18]. The concentrated brine stream is disposed of and another stream of saline water follows it, getting purified as the first stream of feed solution was.

The early concepts of CDI were first laid out in the 1960s and 70s. The pioneering work, by Blair, Murphy, and their assistants started off as the "electrochemical demineralization of water" [19]. This process was thought of as an electrochemical process by which carbon - based electrodes with organic surface groups become anion-/cation-selective, thus becoming capable of

5

removing certain ions from water [20] [21] . The original idea was to compete with conventional methods for removing metal ions, such as ion exchange resin towers, without employing chemical regeneration procedures. Johnson and another team of researchers performed parametric studies on the theoretical basis of CDI and different possible electrode materials. Upon performing a cost analysis, he realized the importance of high surface area, stable electrodes [23] [24]. Johnson also made a theoretical breakthrough, realizing the electrical double layer (EDL) was responsible for the ion removal.

The EDL is a transition zone at the interface between the electrolyte and the electronic conductor (the electrode). It is thought to be divided into two parts, the inner, Hemholtz region where the ions cover the electrodes surface, as well as the 'diffusion' region, where the charge is dependent on the surface potential [25] [26]. Johnson then drafted the original take up and release process for desalination [27]. The next year, in 1971, Johnson and Newman teamed up to conduct experiments resulting in the conclusion that ion removal was also related to the electrical capacity of the EDL, the amount of surface area present on the electrodes, and the applied cell voltage [28].

Capacitive deionization as a desalination technique draws significance from the amount of salt that can be extracted from water. A metric that is becoming more common in CDI is the energy per mole of salt extracted (kWh mmol^{-1}) in favor of the energy per gram of salt [29]. This accounts for various salts that may be able to be removed but have different molecular weights than NaCl. Performance can be indicated by relating the number of moles of salt removed to the electrical energy required to do so.

Because salt consists of charged particles, the number of moles of electrons able to be stored in an ideal capacitor/electrode (the capacitance) is directly related to the number of moles of charged salt ions able to be stored. Equation 2.1 quantifies capacitance [30]:

$$C \ = \ \frac{Q}{V} = \frac{\varepsilon \times A}{d} \qquad \text{[Equation 2.1]}$$

Where the capacitance, C, is determined based on the permittivity of the dielectric medium, ε, the area of the capacitor, A, and the distance between the plates/electrodes. Because the distance between electrodes is less than a millimeter, most of the variability comes down to the strength of the electrolyte (the dielectric), and, more importantly, the area of the capacitor. The cell's differential capacitance, C, in Farads can be also be described in the following equation [1]:

$$C \ = \ I\left(\frac{dV}{dt}\right)^{-1} \qquad \text{[Equation 2.2]}$$

where I is the current in Amperes and V is the cell's voltage in Volts. The material's specific capacitance (F g^{-1} or F cm^{-3}) can be determined through cyclic voltammetry [31].

Using a potentiostat, the voltage of the cell can be increased at a steady scan rate, producing a positive response current. Then, if the voltage is reversed and begins to decrease, the response current will flip signs and start creating a profile with a negative response current. In theory, the resulting profile should be symmetrical, and also encompass an area proportional to

the specific capacitance of the system. Rectangular profiles signify proximity to ideal capacitor behavior. Resistance is proportional to the reciprocal of the slope, due to Ohm's Law.

The Poisson - Boltzmann equation governs the electrostatic potential distribution at the charged surface when it is in an aqueous electrolyte solution. It predicts electrostatic interactions between solvated molecules. Thus, it also predicts the potential distribution at the EDL [32] [33]. The modified Donnan model describes the equilibrium cell EDL structure when the surface of the electrode consists of micropores. It models the micropores with overlapping EDLs, something not taken into account by the Guoy Chapman model for EDLs. This modified model says that the pores act as charge reservoirs and are not equal to an equilibrium chemical potential in the system as previously thought [34].

2.3 Performance Metrics

The field of CDI relies on common metrics to describe and asses the desalination process. Common metrics used to characterize material, energy, and throughput include the salt adsorption capacity (or, SAC, measured in mg g^{-1} of electrodes) [35], average salt adsorption rate (or ASAR, measured in mg g^{-1} s) [36], energy consumption per mole of salt removed (in kJ mol^{-1}) [37], energy normalized adsorbed salt (or, ENAS in μmol J^{-1}) [38], and specific energy consumption (in mg J^{-1}) [39] [40] [41].

The salt adsorption capacity is determined by factors such as the potential of zero charge (PZC) and the capacitance. The PZC is a parameter that affects the performance of a CDI cell, as it is the potential at which a carbon electrode will read zero charge [42]. This is directly

8

dependent on the surface chemistry of the electrode and the charges of the functional groups present on that surface. This potential is also influenced by the pH of the electrolyte.

Common metrics have been defined to describe the conditions of CDI performance. Over time, cell architectures have also been defined, in order to classify the setup of CDI systems.

2.4 Various CDI Flow Cell Architectures

The aim of capacitive deionization is to be an energy efficient desalination technology; thus, the energetics of the system greatly affect its desalination performance and thus determine its success [43]. One way to increase cell performance is to optimize the cell architecture. This refers to the physical geometry and setup of the desalination cell. The general CDI cell consists of two electrodes separated by a flow channel. There are several different alterations on this design [9] [9] [43].

Some of the earlier designs of CDI cells are flow-by CDI cells (FB-CDI), with a channel of water flowing between the electrodes, in contact with both the anode and the cathode.

Around the 1970s, the US Department of the Interior published a paper describing a flow-through set up (FT-CDI) [45] wherein water flows directly through the electrodes, orthogonally. In this geometry, the pore network must be continuous and sized so salt ions, not water, are able to get through. While FT-CDI cells may need higher feed pressures, they are usually able to be more compact and usually produce better desalination rates [46]. FB-CDI usually achieves better performance (higher SAC and charge efficiency) than FT-CDI cells due to a lower contact resistance and fewer faradaic, parasitic reactions [47]. These are not to be

9

confused with flow-CDI (FCDI), a design that encompasses a flowing carbon slurry as the electrolyte.

Flow electrodes were first invented in the 60s and employ carbon particle suspensions as the electrolyte. Later, this carbon slurry was used in systems as the electrode, providing an electrically conductive route of charge transportation. A discovery of the true potential of carbon flow CDI (fCDI) came when flow electrodes were separated into two channels by ion exchange membranes in a way that allowed the carbon flow electrodes to circulate and be regenerated [48] [49]. This reduced limitation on the ion uptake capacity. These types of cells are now known for their ability of continuous deionization and high desalting efficiency, the capacitance must be high and the resistance must be low to achieve low energy consumption [50].

In terms of the source of operation, CDI desalination cell energy is supplied either via constant voltage (CV) [51] [52] [53] [54] or constant current (CC) [56] [57] [58]. In constant voltage operation, a significant amount of energy can be recovered, however, it uses a significant amount of energy when compares to constant current [43]. It has also been proven that constant current has a lower energy consumption per ion removed [58].

2.5 Chemical Modification of Capacitive Deionization

The traditional CDI design is often altered in some way to achieve better performance – this includes adding a membrane, using aqueous instead of solid phase electrode, etc. One major flaw in the CDI process occurs during the point in which the cell system changes polarization. At this point, the electrodes desorb previously adsorbed ions while simultaneously adsorbing oppositely charged ions. Because these two technically occur at the same time, there is an issue

10

of co-ion adsorption, the adsorption of ions to an electrode of the same charge. Capacitive deionization with membranes (MCDI) use ion exchange membranes as selective gates towards the ions, limiting unwanted, energy-depleting electrodynamics [60] [61].

There are two different types of membranes, cation-exchange membranes (CEM) and anion-exchange membranes (AEM). These membranes prevent the passage of a certain ion while allowing the permeation of another [62]. The CEM is put in front of the cathode to block the passage of anions while an AEM is put in front of an anode to block the passage of cations. This limits the unfavorable co-ion adsorption effect, a parasitic process [63]. By eliminating this energy loss, the charge efficiency of the cell improves [64]. In 2006, Lee proposed the theory surrounding ion exchange membranes by demonstrating the salt removal rate of MCDI system is 19% higher than that of a conventional CDI system, a claim backed by multiple studies [65] [66] [67] [68] [69]. More recently, Zhao has shown when feed water salinity is below 2 g L^{-1} TDS and effluent TDS is above 0.5 g L^{-1}, an MCDI cell can be more efficient than reverse osmosis [61]. Many common desalination designs use membranes as a part of their set up. For instance, flow CDI cells (FCDI) are able to employ them in a cell that cycles aqueous phase slurry in place of solid state materials [70] [71] [72]. A FCDI cell can desalinate continuously thanks to the individual carbon electrodes, which can be replaced for an increased capacitance.

Another capacitive design would be inverted CDI (i-CDI). This design tackles the diminishing voltage - induced adsorption and desorption cycles that result from continuous cycling and unfavorable carbon oxidation. By enhancing charged functional groups on the surfaces of the carbon electrodes, the cathode can be rendered negatively charged while the anode can be made to be positively charged - inverting the traditional CDI process. This gives an

increased performance stability and limits separation performance loss due to unwanted carbon oxidation [73].

2.6 Deionization with Redox Active Materials

There exists a spectrum in energy storage devices. These can be classified into capacitors, electro-chemical capacitors, batteries, and fuel cells. CDI cell designs fall into the electro-chemical capacitor category, with energy being stored via a double layer between an electrode and an electrolyte. However, different CDI designs can behave more towards the capacitor end or the battery end of the spectrum.

This can be clearly shown in a Ragone plot (Figure 2). Battery behavior would be classified as involving a faradaic reaction, a slower process but with more specific capacitance. Capacitor behavior would involve storage of energy in the electrical double layer - a faster process but with less specific capacitance. This translates on a Ragone plot as capacitors having relatively higher specific power while batteries have relatively higher specific energy [75].
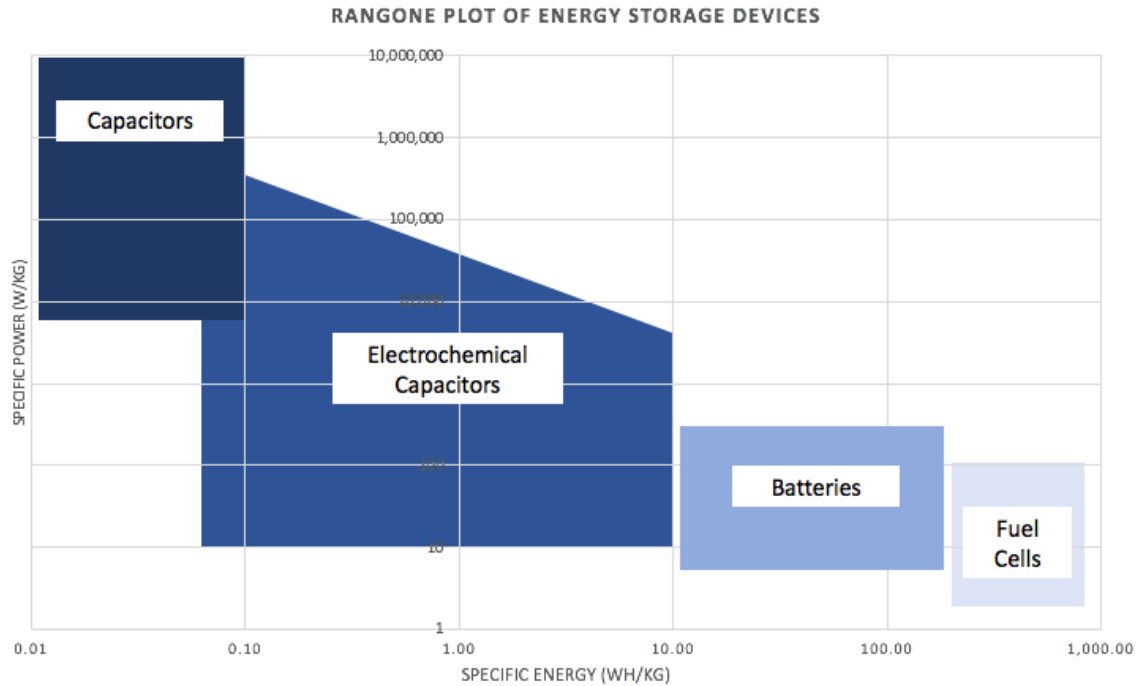
Figure 2: Named after David V. Ragone, a Ragone plot shows how much energy is available versus how fast that energy can be. supplied for various energy storage devices. Both axes are logarithmic. [75] [190].

Conventional CDI cells would fall more towards behaving as an ideal capacitor. This design works using two identical, capacitive activated carbon electrodes. These store charge at the interface of an electrolyte and a carbon electrode, in electrical double layers. Porous carbon material in CDI is chosen for its mechanical support, high surface area, and electrical conductivity. Because surface area of an electrode is such an essential variable in conventional CDI design, much effort is put into electrode material optimization. There are countless high-surface area carbon structures viable for use in CDI cells as well, such as resorcinol-based mesoporous carbon [76], carbon suspension (slurry), carbon nanotube sponges [77] and carbon nanofibers [78]. Using a wet chemical technique called the aqueous sol-gel method, organic chemicals such as resorcinol-formaldehyde (RF) can be treated in a way that, when pyrolyzed,

13

produce a porous, carbon, solid 3D network and therefore extraordinarily high surface areas (from 400 to 800 $m^2 g^{-1}$) [79] [80]. With extremely high surface areas, carbon aerogels can be expected to have a charge storage of around $100 - 200$ F g^{-1} [81] [82].

On the other end of the spectrum lie CDI cells who act more like batteries. In this, CDI cells employ battery materials that allow ions to be captured by chemical bonds instead of the electrical double layer. Battery materials are used because of their high specific capacity and their chemical structure, involving lattices in which ion intercalation is possible [83] [84] [84] [85] [86] [87].

One design that leans far towards battery behavior was pioneered by Pasta and Wessells in 2012, called the desalination battery. This design used an NMO cathode and an Ag/AgCl anode to remove sodium and chloride ions from water. Both sides operate using faradaic principles. The specific capacitance and ion selective properties were an advantage of this design. However, the AgCl's cost and poor electrical conductivity was a major flaw.

Another design leaning towards battery-like behavior is the rocking chair desalination battery, introduced by Seonghwan and Jeyong in 2017 [88]. This design consists of two symmetric faradaic electrodes (sodium nickel hexacyanoferrate (NaNiHCF) and sodium iron HCF (NaFeHCF)) with compartments separated by an anion exchange membrane. Taking inspiration from rocking chair supercapacitor systems, ions move during the charging and discharging steps [89]. However, because the AEM limits cation mobility, charging and discharging the cell further concentrates one compartment while diluting the other. Brine is generated as one cell is desalinated. This system has proven to have such a high desalination capacity that it is able to desalt seawater [88].

Everything in between capacitive and battery-like CDI cells are considered a mixture of the two concepts. Asymmetric system designs work by employing two different types of electrode material, thus being able to take advantage of faradaic material's high specific capacitance while also harnessing the stability, conductivity, and abundance of carbon-based materials.

Hybrid capacitive desalination cells (HCDI), a type of asymmetric design, involve the battery material sodium manganese oxide (NMO, a non-toxic and abundant) and a porous carbon electrode separated by an AEM (Figure 3). The sodium ions are 'captured' in a chemical reaction with the NMO, while the chloride ions can adsorb to the porous carbon surface [2].

$$Na_{x-y} MnO_2 \; + \; yNa^+ + ye^- \leftrightarrow Na_y MnO_2 \qquad [Equation\ 2.3]$$
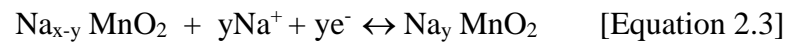
The sodium ions are adsorbed into lattice sites of the faradaic electrode at redox potentials, while the chloride ions are adsorbed into the EDLs of the activated carbon electrode. This set up has been shown to more than double the ion removal sorption capacity seen in conventional cells [68] [90].

15

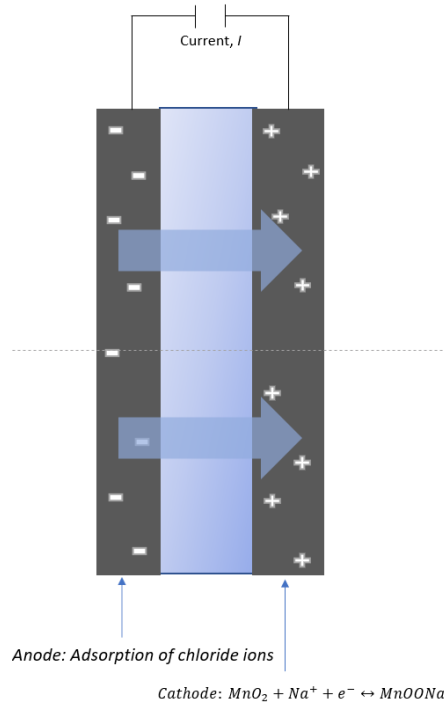$$Cathode: MnO_2 + Na^+ + e^- \leftrightarrow MnOONa$$

Figure 3: A flow - through, hybrid
CDI cell.

CDI cells have electrodes connected in series. Hybrid cell design employs one faradaic

material with higher specific capacitance than the other capacitive material (Figure 3). Because

CDI electrodes are connected in series, the whole cell specific capacitance is a function of either

electrodes individual electrical capacity [60]. This means the cell capacitance is maximized when

either capacitor has an equal contribution - when they are unequal, the total cell capacity is

limited. Therefore, the ratio of the electrode material on either electrode is critical to material

cost optimization.

This ratio can be maximized by increasing the capacitance of the carbon material (by

choosing a material with a large surface area and extensive pore network), or by judiciously

choosing the ratio of faradaic material to capacitive material.

16

2.7 Redox Electrode Materials Employed in CDI

Asymmetrically designed cells and composite electrode material have been made using carbon paired with a carbon/battery material, allowing for the harnessing of multiple material properties. For example, an HCDI system with $AC/Na_4Mn_9O_{18}$ exhibits double the ion sorption capacity of a typical CDI cell (31.2 mg g^{-1} vs. 13.5 mg g^{-1}) [91],

When $AC/Na_2FeP_2O_7$ is used in a HCDI cell, it exhibits a similar deionization capacity (30.2 mg g^1), with an impressive maximum deionization rate performance (0.081 mg $g^{-1}s^{-1}$) [92]. Layer by layer deposition of carbon nanotubes (CNTs)/MnO_2 composite shows an ion adsorption capacity of 80.4 μmol g^{-1}, also showing a high salt removal efficiency (96.8%) [93]. The composite reduced graphene oxide (rGO)/Fe_3O_4 shows a maximum electro sorption capacity prediction of 8.33 mg g^{-1}, roughly twice that of with a pure rGO electrode [94]. The asymmetric system utilizing hierarchical ordered mesoporous carbon (HOMC)/Ag nanoparticles and was able to achieve a 63% increase in comparison to a symmetric electrode [95]. The HCDI system that uses rGO/Co_3O_4 shows an ion removal capacity of 18.83 mg g^{-1}, with an maximum ion removal rate of 0.048 mg $g^{-1}s^{-1}$ [96].

Transition metal oxides, a subsection of battery materials, have been employed in desalination cells. Multitudes of these metal oxides have been employed, such as nickel oxide [97], cobalt oxide [98], ruthenium oxide [99] [100], tin oxide [101] and also manganese oxide [102] [103].

Metal oxides in the form of nanoparticles introduce a higher surface area on the carbon support, thus increasing sorption capacity [104] [105]. Planar metal oxides are also very well

studied, with examples including chemical compounds such as TiO_2 [106], Fe3O4 [107], Al_2O_3 [108], and ZnO [109], [110] [111].

2.8 Phase Transitions and Electrochemical Properties of Manganese Oxide (MnO_2)

While not thoroughly studied in desalination cells, the transition metal oxide MnO_2 shows potential for use in desalination cells. Originally used in electrochemical capacitors (ECs) [112], MnO_2 is a highly stable material that has a relatively large specific capacitance, ranging from 110 to 287 F g^{-1} in its amorphous state [113]. A real advantage of MnO_2, however, is the structural diversity - there are about 30 known polymorphs of this mineral, including crystal structures and various chemistries that have the potential to be used for ion removal in HCDI cells [114]. Manganese oxide also consists of a redox pair with high electrochemical activity, Mn^{3+}/Mn^{4+}, and therefore high ion removal capacity [115] [116].

The transition metal manganese oxide (MnO_2) is capable of storing Na^+ from aqueous electrolytes - with the stoichiometric ratio between Na^+ to MnO_2 being 1 to 1 instead of 4 to 9 as seen in previous studies with sodium manganese oxide [3] [117] [118]:

$$MnO_2 \ + \ Na^+ + e^- \leftrightarrow MnOONa^+ \qquad \text{[Equation 2.4]}$$

A lower ratio is more favorable in terms of MnO_2 material cost. This cation intercalation happens during the reduction of the electrode and de-intercalation that happens upon oxidation of the electrode [119]. In electrochemical desalination cells, MnO_2 - coated porous carbon electrodes have a large ion storage capacity but undergoes significant volumetric changes with

18

charging and discharging. To counteract this cycle instability, synthesis is often in the form of thin films, nanowires, spinels, and crystalline structures [120] [121].

The relevant original phase for the MnO_2 used in this study is amorphous, as its chemical structure is unordered. Electrochemical property shifts, such as increased capacitance or selectivity, accompany the phase transition from amorphous to crystalline MnO_2. One objective of this work is to facilitate that phase transition.

These transitions can be coerced by wet chemical ion exchange and heat treatment. Both Sassin and Donakowski demonstrated that in Na^+ - MnO_x, topotactic ion exchange of interlayer Na+ to Li^+ eventually will, upon heat addition, give way to a 3D extended, spinel, lithiated phase ($LiMn_2O_4$@CNF). The effects are shown in the cyclic voltammograms of either paper (Figure 4), which demonstrate the facilitation of redox reactions and the resultant increase in specific capacitance.

2.9 Various Manganese Oxide Fabrication Techniques

Various synthesis methods have been used to tailor favorable characteristics of MnO_2. By utilizing an ultrasonic assisted wet-chemistry fabrication technique, MnO_2 can be confined within carbon nanotubes - resulting in a material with impressive electrochemical reversibility and a specific capacitance of 225 F g^{-1} [122]. A slightly greater specific capacitance of 292 F g^{-1} can be achieved by nano structuring MnO_2 using the one pot strategy [123]. Layered deposition of MnO_2 also results in an exceptional specific capacitance (345 F g^{-1}), in addition to resulting in improvement of electrical conductivity [93]. Very little volume expansion is observed across cycling when MnO_2 nanoparticles are used to enriched polymer nano wires. This material also

19

exhibits high conductivity, as well as a noteworthy specific capacitance (410 F g^{-1}) (Liu & Duay, 2010). Electrodeposition of mesoporous MnO_2 minimizes volume changes across repeated cycling as well, leading to incredible stability and thus the ability to retain 98% of its capacity after 10,000 cycles [3] [124]. Electro-less deposition coating of amorphous MnO_2 onto porous nanofoam via self-limiting reaction produces a high surface area interface between nanoscopic MnO_2/carbon nanofoam; this leads to a large reversible capacity (801 mA h $g-1$), as well as good cycling stability (no capacity fade in first 20 cycles) [125] [126] [3].

Electro-less deposition is a fast, reproducible, financially feasible way to deposit metal nanoparticles and polymers onto activated carbon. It is autocatalytic and simply requires a substrate be dipped in the electro-less solution containing the metallic ions.

The electro-less deposition of permanganate onto a carbon nanofoam is a self-limiting redox reaction that acts to deposit macroscopic levels of amorphous MnO_2 onto a nanofoam substrate. The MnO_2 is able to infiltrate and react with the surface and pores of the carbon nanofoam. As the internal MnO_2 coating grows thicker with increased deposition times, the average pore size shifts to smaller sizes and the overall pore volume decreases. The pseudo capacitance of the composite has also been proven to increase with deposited MnO_2 [127]. Inventor and prominent researcher Anne E. Fischer filed a patent on this procedure in 2007 (EP2061607A2 with the European Patent office).

Recent research of the electro-less deposition of MnO_2 onto porous carbon as it relates to capacitance, and optimized performance parameters. In Hand's work, increased electro-less deposition time leads to an increase in capacitance and maximization of performance parameters such as sodium adsorption. However, with increased electro-less deposition times, there are

diminishing returns [3]. The effect of deposition times of MnO_2 has yet to be related to other electrochemical properties. This work will explore its effects on ion selectivity.

2.10 Ion Selectivity

The chemical nature of metal oxides plays a large role in ion selectivity. For one, the lattice geometry and degree of crystallinity is influential in the selective nature of such chemical compounds. CDI systems that exhibit ion selective properties towards multi ion solutions have applications in water softening [128] , contaminant ion sieves [129], and heavy metal ion removal [130]. While lithium battery materials (LIBs) and their lithium ion-selective nature have been investigated [131] [86] [132], sodium ion battery materials, such as sodium manganese oxide, have not been studied as much.

Sodium manganese oxide ($Na_{0.44}MnO_2$) and various phases of MnO_2 have been shown to selectively separate Na^+ and other cations from mixed solutions [133] [134]. Ion selectivity has been linked to the chemical charge of the ion being adsorbed, lattice site size, hydrated radius, and initial molar concentration [135] [136] [137], with the preference being for monovalent ions.

Hydration shells are a good prediction of the actual size of various ions. Because electrolytes dissociate in aqueous solutions, the intercalation ion will be charged and hydrated. Therefore, the intercalating ion will have a hydrated radius which is many times the size of the anhydrous ion. For the electrolytes KCl, NaCl, LiCl, and $CaCl_2$, hydration shells mean the intercalated ion size goes (in ascending order) $K^+ < Na^+ < Li^+ < Ca^{2+}$ [138] [139] [140] [141].

Diffusion coefficients, with units in $cm^2\ s^{-1}$, help to quantify the diffusion of aqueous ions in a solution due to molar flux and molecular diffusion. The larger the diffusion coefficient, the less resistance it experiences. The acceding order for the aforementioned list of ions goes [139] $Ca^{2+} < Li^+ < Na^+ < K^+$. Interestingly enough, the order of the ions is exactly reversed. Therefore, the smaller the ion, the less resistance it experiences due to molecular diffusion.

In this study, we characterize the performance of MnO_2 - coated porous carbon aerogel electrodes while varying procedural fabrication. The various conditions help to see the progress (or lacktherof)) from phases to phase. We perform Li^+ - ion exchange and heat treatment on the amorphous MnO_2 phase, in order to create a lithiuated, crystalline structure with increased capacitance and ion selectivity capabilities. Additionally, we will vary the electro-less deposition in order to optimize capacitance and eventually performance parameters. By varying the electrolytic solution (Na^+, Li^+, Ca^{2+}, K^+), we can study the cathode's faradaic ion uptake mechanism and the factors influencing it across these various electrode fabrication conditions. Future work involves the optimization of operation parameters such as flow rate, current density, and molar concentration once the optimized aerogel electrodes can be incorporated into a hybrid capacitive deionization cell.

CHAPTER 3: MATERIALS AND METHODS

3.1 Electrode Synthesis

In order to explore various fabrication conditions and their results on ordered, Li^+ - deposited, MnO_2 - coated carbon aerogels , a matrix of experimental conditions was created, then systematically tested (Table 1). These conditions are outlined below.

Table 1: A matrix outlining the various carbon aerogel fabrication conditions. There were four variables of fabrication – deposition time, lithium ion exchange, and heat treatment. Two controls were also fabricated. These experiments were all in triplicate.

Condition	MnO_2 deposition time	Li+ deposition	Heat to 300 °C under Ar (g)
1	15	+	-
2	240	-	-
3	15	+	-
4	240	-	-
5	15	-	+
6	240	+	+
7	15	+	+
8	240	-	+
9	none	-	-
10	none	-	+

Phase 1: Electro-less deposition

Precursor carbon aerogels (Type I, Marketech International, USA) were vacuum filtrated with 0.1 M Na_2SO_4 overnight to wet all the aerogel pores [142]. The aerogels were then

coated via electro-less deposition using 0.1 M Na_2SO_4 and 0.1 M Na_2MnO_4 for durations of either 15 or 240 minutes (ED15 or ED240) [3]. The carbon substrate acts as a reducing agent in converting aqueous permanganate (MnO_4^-) to insoluble MnO_2. The result is deposition of nanoscale MnO_2 throughout the 3D porous carbon aerogel network. The aerogels were subsequently left under nitrogen for four hours. Deposition was done to conditions 1 – 8. Only deposition was done to 2 and 4.

Phase 2: Ion Exchange

The carbon aerogel electrodes were then soaked in aqueous 1 M $LiNO_3$ for 24 hours at 25 °C to exchange Na^+ ions for Li^+ ions. After rinsing, they were placed under vacuum for 2 hours and then under flowing N_2 (g) at 50 °C for 12 hours [143]. Conditions 1, 3, 6, and 7 experienced lithium deposition.

Phase 3: Heat Treatment

The electrodes were heat treated to convert the amorphous structure to crystalline structure. Briefly, the electrodes were placed under flowing argon at 2 °C per minute to 300°C for 4 hours in a tube furnace. Afterwards, the electrodes were placed in a muffle furnace under static air at 200 °C for 6 hours. This was done under flowing N_2 (g) [144] [143]. Conditions 5 – 7 and 9 experienced heat treatment.
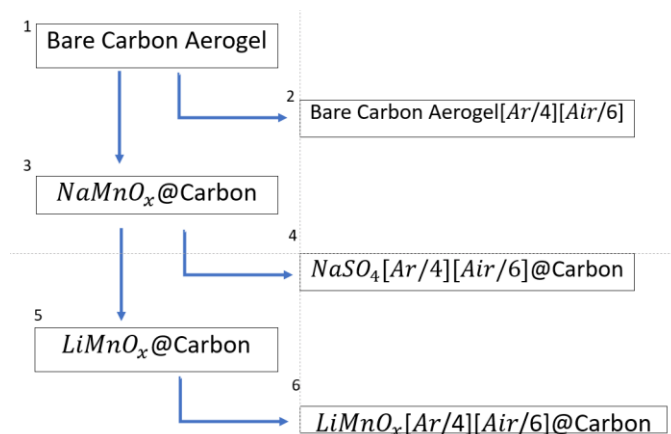
Figure 4: The treatment process of the aerogels. The bare carbon aerogel (1) underwent MnO_2 deposition then underwent Li^+ ion exchange. The resulting products were then heat treated.

3.2 Characterization

The deposited aerogels were characterized in terms of chemical composition and pore size distribution. For the elemental makeup of the sample, thermogravimetric analysis (TGA) (PerkinElmer Pyris 1, USA) was performed on the sample. In order to find the surface area of the aerogel per unit mass, the Brunauer, Emmett, and Teller (BET) analysis was performed (Micromeritics ASAP 2020, USA). Electrochemical performance of the deposited aerogels was determined with cyclic voltammetry. Cyclic voltammetry was done using a potentiostat (Biologic VMP3, France) and a three-electrode system with 0.1 M electrolytic solutions ($NaCl, KCl, CaCl_2, LiCl$). The reference electrode was KCl saturated $Ag/AgCl_2$, while the counter electrode was dimensionally stable ruthenium metal oxide coated titanium. The voltage window

25

ranged from -0.1 to 0.8 V. All of the cycles taken were repeated several times to more accurately record the system's state.
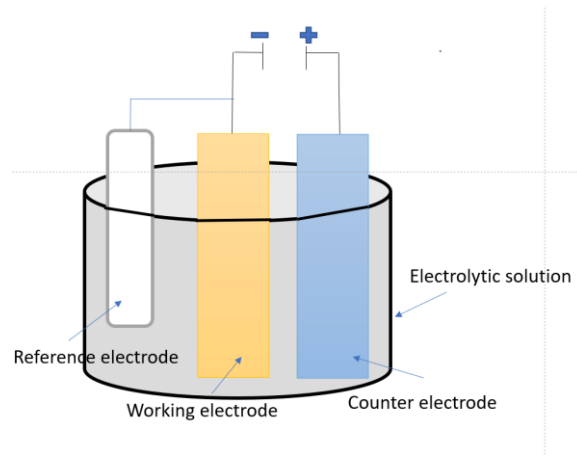

Figure 5: A three - electrode set up. The circuit dynamics are output using a potentiostat.

CHAPTER 4: RESULTS AND DISCUSSION

4.1 Physical Characterization

BET analysis was done on the carbon aerogel with an MnO_2 deposition time of 15 minutes. This provided information on surface area per mass of MnO_2 (Table 2). It was found to be much lower than previous literature values of the same material and deposition time. On the other hand, the thermogravimetric analysis resulted in the MnO_2 content being almost twice as much as previous literature values of the same material and deposition time. These physical characterization results imply the MnO_2 deposition rate was higher than previously reported values [3].

Table 2: The physical characterization of carbon aerogels when deposited for 15 minutes. Values were compared to Hand's characterization of the same material [3].

Technique	Information sought	Parameter	Literature Value
BET Analysis	Area / mass ($m^2 \ g^{-1}$)	170	399
TGA	MnO_2 content	14.64%	6.90%

4.2 Electrochemical Characterization

To observe their electrochemical properties, each fabricated electrode was placed in a three - electrode set up, done with each of the various electrolytic solutions. The resulting cyclic voltammograms (CVs) give information on the electrochemical responses of the electrodes - this helps to characterize the electrode material. The graphs presented are the curves produced only

27

after the system ran for three or four cycles. The graph below (Figure 6) shows the cyclic

charging behavior of the bare carbon aerogel control, in which no deposition, ion exchange, nor

heat treatment occurred. The y - axis has been formatted to show the specific capacitance,

however, raw cyclic voltammograms are of the current produced versus the potential applied

between the working and reference electrode. This acts as a capacitance baseline. As we can see,

the variance in the electrode capacitance when exposed to different electrolytic solutions is

nominal indicating that the electric double layer storage mechanism of the aerogel did not exert
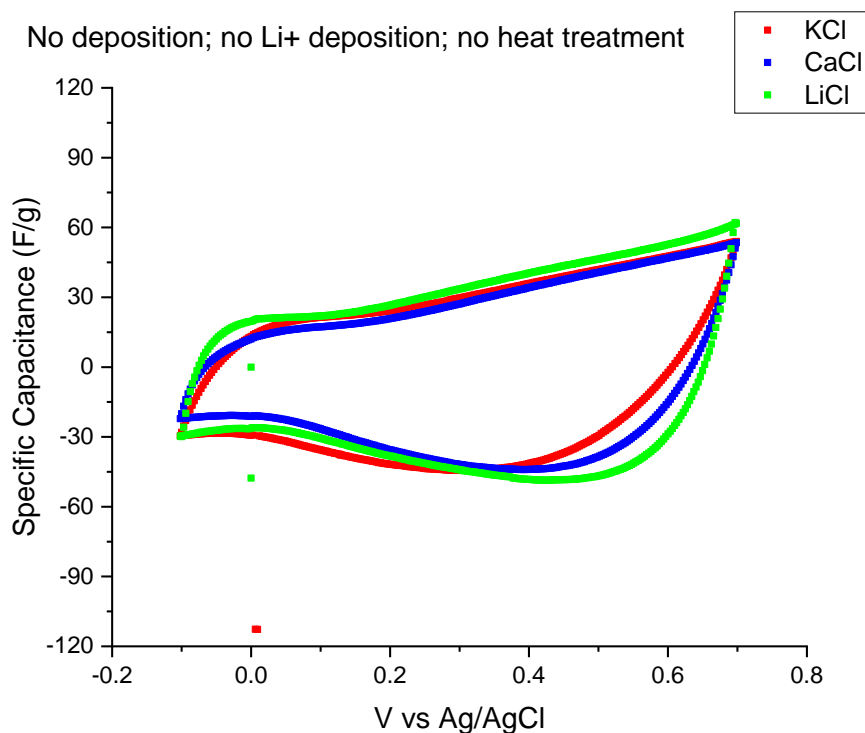
ion-selectivity.

Figure 6: This CV is of the bare carbon aerogel. NaCl is not included in this graph due to
unsatisfactory noise in the signal.

28

The next graph (Figure 7) is of the bare carbon aerogel after 15 minutes of Mno$_2$ deposition. At this level of treatment, Hand's specific capacitance increased from 36 F/g for a bare carbon aerogel to 47 F/g after 15 minutes of deposition. A 31% increase attributable to the 15-minute deposition. For this study, the average specific capacitance across all electrolytes went from 47.6 F/g with no treatment to 71.9 F/g with 15 minutes of deposition. That's a 51% increase. This means that there was a larger increase in specific capacitance attributable to the 15-minute deposition time than expected.

As for ion selectivity, the electrolyte impact on the capacitance of the cycle profiles is insignificant, as all the CV profiles are roughly identical in shape and profile. The rectangular nature of the profiles implies that the ions were stored largely capacitively in the rather shallow MnO$_2$ coating.
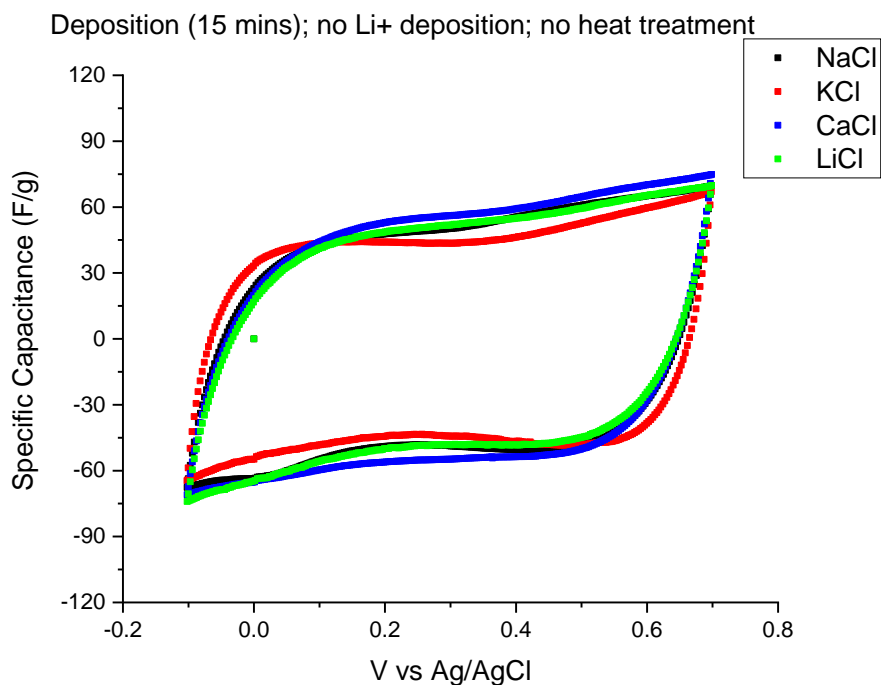

Figure 7: The changes in specific capacitance due to electrolyte are nominal in this graph as well.

29

Below, Figure 8 shows the profile of a carbon aerogel having undergone electro-less deposition for 15 minutes as well as being heat treated. The deposition of a relatively small amount of amorphous faradaic material would be expected to slightly increase capacitance, while increasing the resistivity due to the addition of the low conductivity oxide layer. While there is no significant difference between electrolytes, the average specific capacitance for this with both deposition and heat treatment is 74.5 F/g. This shows a small, 3.6% increase in capacitance from an aerogel with deposition but no heat treatment. This implies this small jump in capacitance is due to the heat treatment.

Once again, the CV profile and capacitances have no discernible relationship to the electrolyte solution. The profile is rather rectangular again, implying a largely capacitive ion storage mechanism.
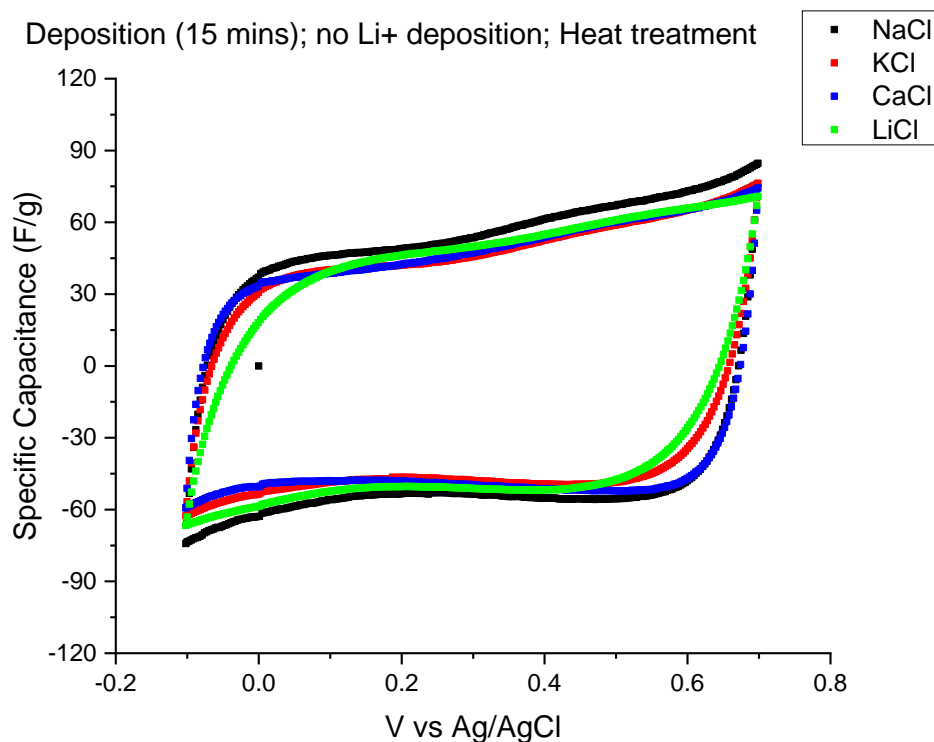
Figure 8: The Na$^+$ - deposited and heat - treated electrodes. No redox peaks are observed across this voltage window, implying the absence of faradaic reactions.

The CV in Figure 9 (below) is for a carbon electrode that has undergone 240 minutes of electro-less deposition as well as lithium deposition. It did not go through heat treatment. For this level of treatment, the average specific capacitance shown is 87.53 F/g, whereas Hand's paper shows a value of 92.8 F/g for 240 minutes of deposition alone. Going by that literature value, there was either a decrease in capacitance or no effect on capacitance due to the lithium deposition.

Additionally, the profile looks more feather-shaped than rectangular. Increased resistivity of this profile be attributed to the low conductivity of the metal oxide layer deposited for a lengthier amount of time [145] [146]. No relationship between ion selectivity is observed across the electrolyte solution. Redox peaks aren't present in this voltage window either.

31

In this CV (Figure 9), the profile of the CaCl$_2$ electrolyte is larger than the other profiles. This could imply ion selectivity at this level of treatment; however, it is not exhibited in any of the other CVs. Additionally, when comparing the numeric specific capacitances across electrolytes, the averages are NaCl > CaCl$_2$ > KCl > LiCl. This profile in which the CaCl$_2$ is much larger than the other profiles can be attributed to experimental variability.
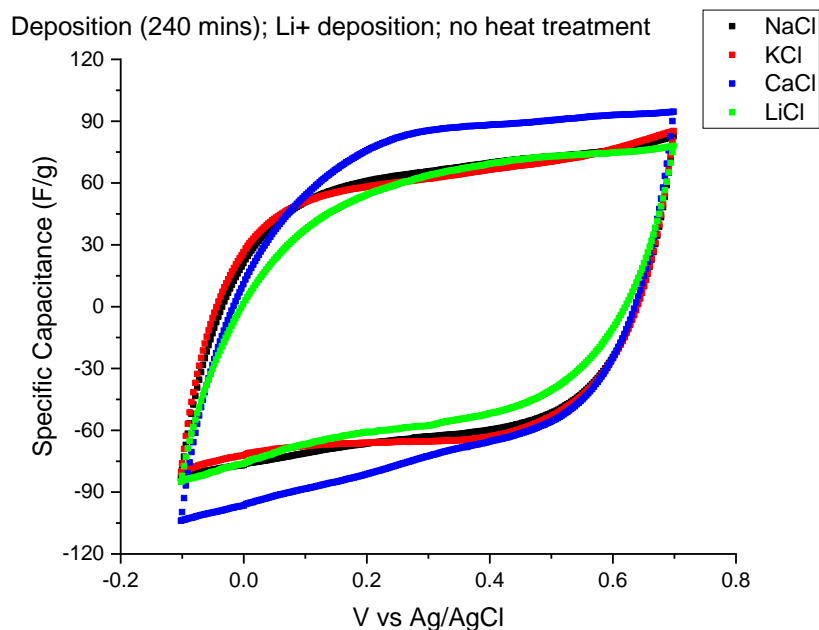

Figure 9: The MnO$_2$ deposited and heat treated electrodes. No redox peaks are observed across this voltage window, implying the absence of faradaic reactions.

The final graph, (Figure 10) shows an electrode that has undergone all conditions of treatment, with a deposition time of 240 minutes. The average specific capacitance is 72.5 F/g. This value is also lower than Hand's value for an aerogel only having underwent a 240-minute deposition, implying the lithium deposition and heat treatment condition led to a decrease or had no effect on the specific capacitance.
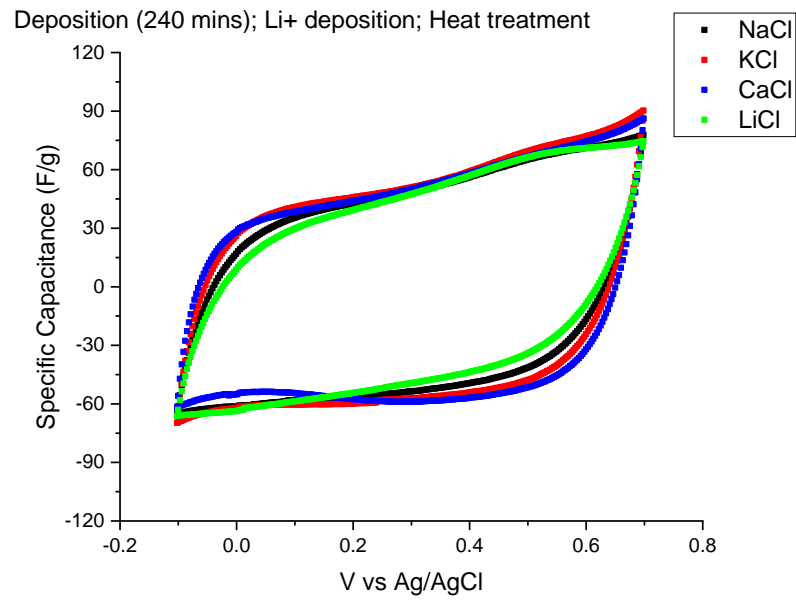
Figure 10: The increase in resistivity and average specific capacitance is thought to occur due to less hydration shells.

CHAPTER 5: CONCLUSIONS AND RECOMMENDATIONS

The purpose of this study was to investigate the relationship between electrode fabrication techniques and the resulting effects on ion selectivity and specific capacitance. More specifically, carbon aerogels were coated in MnO_2, subject to a Li^+ - ion exchange technique, and heat treated with the purposes of activated a more ordered, crystalline phase capable of ion selectivity and higher specific capacitance. There were three main conclusions.

Firstly, the aerogel that was subject to 15 minutes of electro-less deposition experienced a higher rate of MnO_2 content deposition than previous studies (at 399 $m^2 g^{-1}$ vs 170 $m^2 g^{-1}$ [3]). The second conclusion was that on average, across all electrolytic solutions, there was an increase in specific capacitance from bare carbon aerogel to treated aerogel (be it electro-less deposition, ion exchange, and/or heat treatment). Lastly, because specific capacitances are approximately the same at low and high electro-less deposition times, the optimized duration should last for 15 minutes instead of 240 minutes.

In terms of future works, the further characterization of the aerogels used in this study can help to identify the extent to which the heat treatment ordered the structure as well as the extent to which the Na^+ ion interlayer was replaced with Li^+ ions. This would be a start in explaining the mechanism or lack thereof in the aerogel behavior. As for the HCDI desalination cell, a new design should be able to employ the aerogel system with the desalination set up of a CDI cell without shorting the circuit, while simultaneously avoiding shattering and cracking the aerogel due to the applied pressure from the side plates.

CHAPTER 6: EDUCATIONAL OUTREACH

6.1 Overview of Exercise

The goal of this educational exercise was to provide students a hands-on experience of how environmental engineers use physics, chemistry, and math to improve the quality and safety of drinking water. Students were required to build and evaluate granular and membrane-based filtration devices to filter 'contaminated water'. 'Contaminated' meant it just had orange dye and small dirt particles inside, a way to symbolize dissolvable and undissolvable contaminants. During the activity, they were to time the filtrations as a way to compare the membrane vs granular filters.

This was done on two separate occasions, to different groups of school students. The agenda for the lesson plan involved discussion, a short PowerPoint presentation, as well administering short quizzes to assess knowledge progression and retention. The topics covered were:

- Classifying water quality

- Relative sizes of varying water pollutants

- The Chicago water cycle

- The advent of water quality regulations in the U.S.

- Introduction to chemical and physical water treatment methods

- Introduction to various types of filters (membrane, granular/sand, and activated carbon)

Site Visits:

STEM Day 1

Date: February 19th, 2019

School: Betty Shabazz International Charter School

Location: 7822 S Dobson Avenue

Chicago, IL 60619

Audience: 32 middle school students (5th - 8th graders)

STEM Day 2

Date: April 25th, 2019

School: Franklin Middle School STEAM Academy

Location: 817 N Harris Avenue

Urbana, IL 61820

Audience: 11 middle school students (5th - 8th graders)

6.2 Student Procedure

Students were broken into small groups. Each group made and tested a sand filter (either rapid or slow) and membrane filtration device. Instructions for the slow sand filter were as follows:

1. Gather a pop bottle with a cap and two filter cloths.
2. Put the filter cloth on the mouth of the bottle and screw on the top. Hold it upside down, like a funnel. Don't shake it.

3. WITHOUT shaking it or spilling the rocks, put 20 mL of both large and medium pebbles inside, then a light coating of small black pebbles.

For the rapid sand filters, the procedure is the same except the pebbles are larger. When time to assemble the pre-ordered membrane filtration devices, the instructions were as follows:

1. Place a beaker on the table.
2. Hold the blue and black membrane syringe so that the label that says 'flow' points into the cup.
3. Screw the bag on the top of the membrane filter.

Afterwards, the students were to record the time to filter, in seconds, and the volume of water produced, in mL. It was presented as a fill in answer:

Time to filter _____ s, Volume of water produced _____ mL

When the data collection was complete, groups with sand filters were to switch with groups with membrane filters and collect the filtration time and volume produced again. After everyone was done collecting and averaging their data, they were to fill out a data summary chart included in the Appendix. This chart helps them to find the overall filtration rate for both types of filters.

The activity was modified for STEM Day 2 in response to the audience of students as well as due to observations made during STEM Day 1. The second group is known to be more energetic, talkative, and include younger participants. The procedure was modified in the following ways:

- There was no written data collection
- Students had a discussion and volunteered to answer questions in lieu of getting a post quiz
- Instructions were not written and followed by the students. Instead, I walked the entire class through each step for both filters.
- The presentation was shortened

Both groups received the same quizzes. Location I had a written pre and post quiz, while location II wrote the pre quiz and discussed answers for the post quiz. The questions were:

1. Do you know where Chicago gets its drinking water from?
2. Who sets the water quality standards for our drinking water?
3. Can you see yourself possibly studying engineering/science in the future? Why or why not?

6.3 Results

For location I, Betty Shabazz Academy (BSA), the results of the pre and post quizzes tests are as follows:
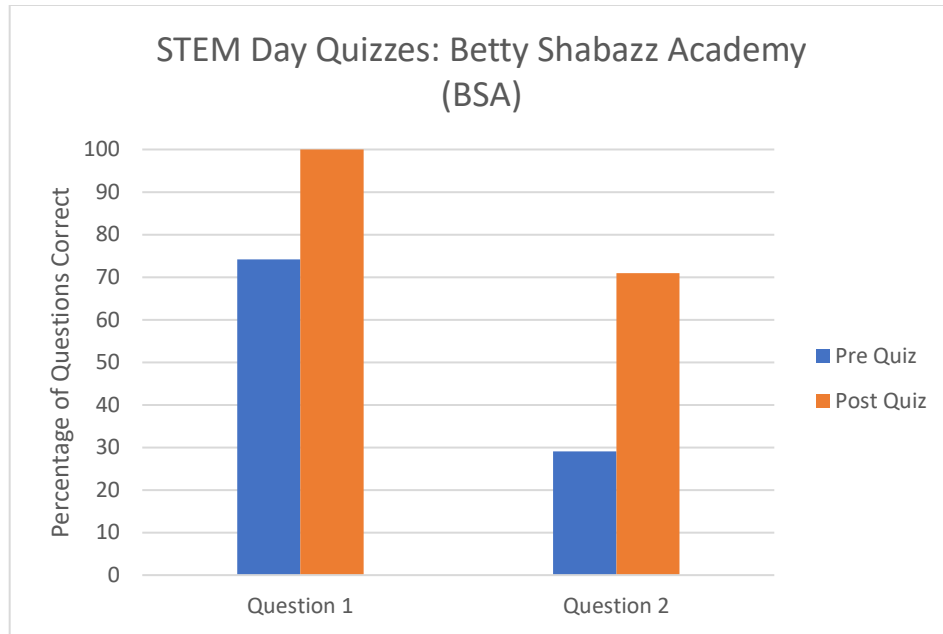
Figure 11: There were 32 students that filled out the survey.

There was a significant increase in the number of correctly answered questions at the first

location (Figure 11), Betty Shabazz Academy (BSA). This success can be attributed to the length

of the presentation being reduced from 15 minutes to 5 minutes, as well as the relevancy of the

information presented. These students lived in Chicago, so explaining the system they already

interacted with was interesting to them. They remained engaged through the entire oral

presentation.

Question 3 asked about the likelihood of the student going into a STEM field. The results are

below (Figure 12). This shows that the number of students believing they can go into STEM

increased due to the lesson (going from 41% to 48%). Meanwhile, the number of students

answering maybe/no decreased due to the presentation (going from 22% to 7%).
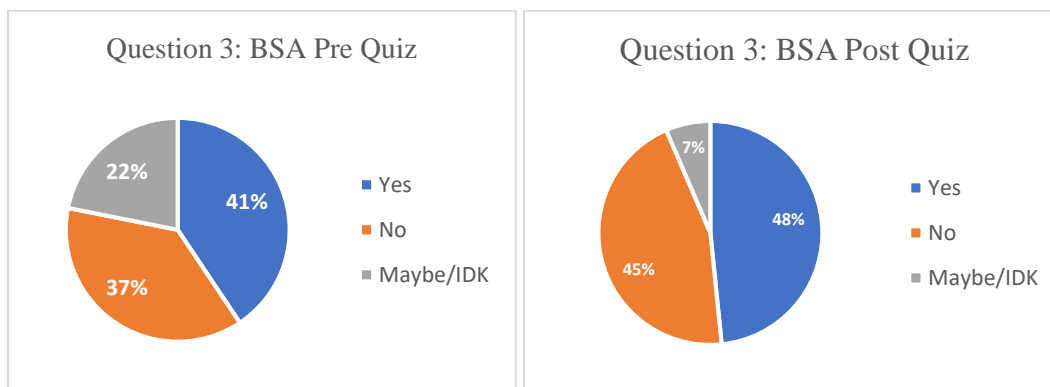
Figure 12: Students become more decisive and more confident in their ability to go into STEM.

As for Franklin Middle School STEAM Academy, no post quizzes were given, in lieu of a group discussion. The amount of students who answered the pre quiz at Franklin Middle School (10 students) was significantly lower than those who answered at Betty Shabazz (31 students) (Figure 13). This could be due to the fact the information wasn't local. The presentation was centered around Chicago water cycles. Additionally, the presentation was considerably shorter due to time constraint.
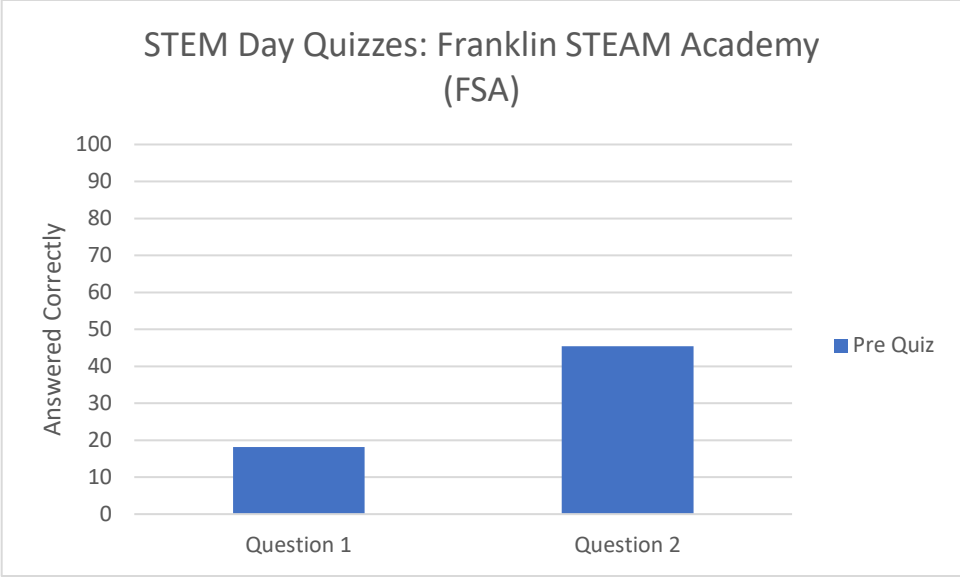
Figure 13: The pre quiz given to the students show relatively low numbers of correct

Question number 3 asks if the students have confidence in the STEM subjects. The distribution shows the group at Franklin was relatively indecisive (Figure 14).
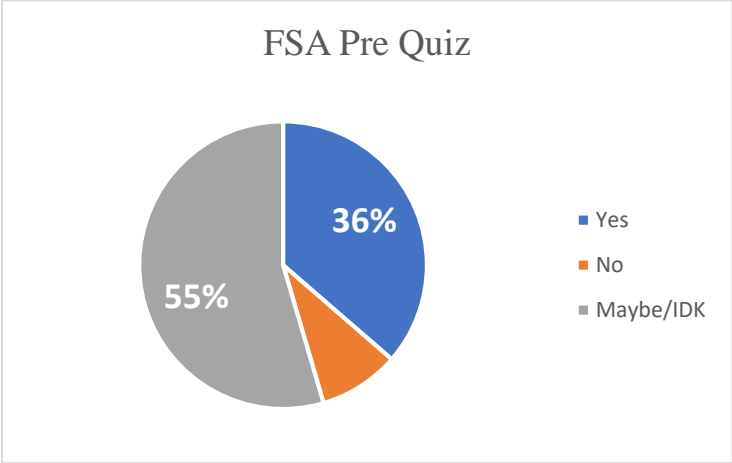

Figure 14: The total number of students screened was 11.

Group discussion showed several students extremely interested in answering the first two questions, evident by the number of raised hands. As for question 3, regarding confidence, the students seemed confident enough. Most of the class raised their hands as being confident enough to pursue STEM as a career.

6.4 Observations and Discussion

During the lesson plan presented at BSICS, there were several observations to be made during the activity. The students naturally presented a wide range of learning styles. The ways the children began to grasp the concepts spanned from reading the instructions thoroughly, tinkering with the materials provided, or a mix of both. Additionally, as the activity went on, weak points in the lesson plan arose. For instance, the lesson plan took about 15 minutes over time. The observations noted are outlined below.

- Students were able to deduce further concepts by tinkering with the filters. For example, one group continued to use their sand filter to filter the water, and after a certain amount of time, even when dirtier water was used, the filter performed better. This is because the gaps in the media had approached optimal pore size, thus increasing the filter's ability to capture particles at this media's size. The group made this observation on their own.

- This age group did not bother to read the instructions once the materials and devices were in front of them. In the future, the instructions should be read and then the materials passed out afterwards.

- More time is necessary for the hands-on portion at BSA. We were 15 minutes over the allotted time.

- The children understood all concepts, more advanced topics could be explored

- When explaining how we know water is dirty, many students mentioned indicators that extend beyond our senses, such as pH indicating an understanding of chemical concepts.

- The question on whether or not the students could see themselves in engineering or science may not have been fully understood. Several students answered no, and instead said something that still falls under the STEM category. Example of a post quiz: "No, because I want to do computer science or mathematics".

Observations made during the modified lesson presented to location II (Franklin STEAM Academy) are as follows:

- Assembly of the filters went smoothly when the class went through the instruction steps together

- Having a volunteer stay at a table with each group kept the students on task, as opposed to several volunteers walking around helping those who called for help.

- The session was done 15 minutes early, including clean up time. This is probably due to the shortened presentation or the lack of written post quiz.

- During the post discussion, students fully understood the time differences and physical specialties of each filter.

- Not as much input from more reserved or withdrawn students during discussion. This is probably because discussion was optional, whereas a written quiz would have been more mandatory.

- Students at this location also began re-filtering the contaminated water through the granular filters and also noticed the effects of approaching optimal pore size. This was unprovoked.

By presenting information about science in an engaging and hands on environment, students can learn topics in a way that makes the experience more memorable and educational. It also sparks students' interest when a familiar topic is presented as an application to real world problems. Future works involve conducting this demonstration at various schools in the greater Chicagoland area, altering the technical nature of the content in accordance with the location of the event, as well as the maturity and background of the students.

REFERENCES

[1] "Capacitors," 09 May 2019. [Online]. Available: http://www.elna.co.jp/en/capacitor/double_layer/principle/index.html.

[2] C. Zhang and D. Waite, "Faradaic reactions in capacitive deionization (CDI) - problems and possibilities: A review," *Water Research,* pp. 314-330, 2018.

[3] R. C. S. Hand, "Characterizing the Impacts of Deposition Techniques on the Performance of MnO2 Cathodes for Sodium Electrosorption in Hybrid Capacitive Deionization," *Environmental Science and Technology,* 2017.

[4] "OECD Environmental Outlook to 2050," 2012. [Online]. Available: www.OECD.org.

[5] M. B. L. A. K. N. M. Shahzad, "1 - Adsorption desalination—Principles, process design, and its hybrids for future sustainable desalination," in *Emerging Technologies for Sustainable Desalination Handbook*, Butterworth-Heinemann, 2018, pp. 3-34.

[6] D. L. L. Greenlee, "Reverse osmosis desalination: Water sources, technology, and today's challenges," *Water Research,* pp. 2317-2348, 2009.

[7] S. H.-Y. Y. Ting-Hua, "Life cycle assessment of environmental impacts and energy demand for capacitive deionization technology," *Desalination,* pp. 53-60, 2016.

[8] M. Anderson and A. Cudero, "Capacitive deionization as an electrochemical means of saving energy and delivering clean water. Comparison to present desalination practices: Will it compete?," *Electrochimica Acta,* pp. 3845-3856, 2010.

[9] P. B. L. Wang, "Reversible thermodynamic cycle analysis for capacitive deionization with modified Donnan model," *Journal of Colloid and Interface Science,* pp. 522-528, 2018.

[10] S. P. H. d. G. K. Singh, "Timeline on the application of intercalation materials in Capacitive Deionization," *Desalination,* pp. 115-134, 2015.

[11] M. Kummu and J. Guillaume, "The world's road to water scarcity: shortage and stress in the 20th century and pathways towards sustainability," *Scientific Reports,* p. 6, 2016.

[12] M. Mekonnen and A. Hoekstra, "Four billion people facing severe water scarcity," *Science Advances,* 2016.

[13] P. Gleick, Water in Crisis: A Guide to the World's Fresh Water Resources, New York: Oxford University Press, 1993.

[14] F. Chen and Y. Huang, "Dual-ions electrochemical deionization: a desalination generator," *Energy and Environmental Science,* pp. 2081-2089, 2017.

45

[15]   P. Simon, Tapped Out: The Coming World Crisis in Water and What We Can Do About It, Welcome Rain Publishers, 2001.

[16]   N. Mazlan and D. Peshev, "Energy consumption for desalination—A comparison of forward osmosis with reverse osmosis, and the potential for perfect membranes," *Desalination,* pp. 138-151, 2016.

[17]   T. Yu, H. Shiu and M. Lee, "Life cycle assessment of environmental impacts and energy demand for capacitive deionization technology," *Desalination,* pp. 53-60, 2016.

[18]   J. J. A. Subramani, "Emerging desalination technologies for water treatment: A critical review," *Water Research,* pp. 164-187, 2015.

[19]   T. Welgemoed and C. Schutte, "Capacitive Deionization Technology: An Alternative Desalination Solution," *Desalination,* pp. 327-340, 2005.

[20]   B. JW and M. GW, "Electrochemical demineralization of water with porous electrodes of large surface area," *Saline Water Conversion,* pp. 206-223, 1960.

[21]   B. Arnold and G. Murphy, "Studies on electrochemistry of carbon and chemically modified carbon surfaces," *Journal of Physical Chemistry,* pp. 135-138, 1961.

[22]   A. Fischer and K. Pettigrew, "Incorporation of homogeneous, nanoscale MnO2 within ultraporous carbon structures via self-Limiting electroless deposition: implications for electrochemical capacitors," *Nano Letters,* pp. 281-286, 2007.

[23]   A. Johnson, "Electric demineralization apparatus," *US Patent,* 1973.

[24]   Y. Oren, "Capacitive deionization (CDI) for desalination and water treatment — past, present and future (a review)," *Desalination,* pp. 10-29, 2008.

[25]   B. JOM and R. AKN, "Modern Electrochemistry 2B: Electrodics in Chemistry, Engineering, Biology and Environmental Science," *Kluwer Academic Publishers,* 2000.

[26]   B. Jia and W. Zhang, "Preparation and Application of Electrodes in Capacitive Deionization (CDI): a State-of-Art Review," *Nanoscale Research Letters,* 2016.

[27]   A. Johnson , A. Venolia and J. Newman, "Electrosorb process for desalting water," Office of Saline Water Research and Development, Progress Report No 516, US Department of the Interior, 1970.

[28]   A. Johnson and J. Newman, "Desalting by means of porous carbon electrodes," *Jounral of the Electrochemical Society,* pp. 510-517, 1971.

[29] J. D. L. Wang, "Energy Efficiency of Capacitive Deionization," *Environmnetal Science and Technology,* 2018.

[30] M. Hill, University Physics, Wolfgang Bauer & Gory D. Westfall, 2011: Physics Volume 1 of University Physics, Bukupedia, 2011.

[31] A. Bard and L. Faulkner, Electrochemical Methods, New York: John Wiley & Sons, 2001.

[32] P. Pham and M. Howorth, "Numerical Simulation of the Electrical Double Layer Based on the Poisson-Boltzmann Models for AC Electroosmosis Flows," in *COMSOL Users Conference*, Grenoble, 2007.

[33] J. Hsu and M. Tseng, "Solution to linearized Poisson–Boltzmann equation with mixed boundary condition," *Journal of Chemical Physics,* 1996.

[34] S. Porada and M. Bryak, "Effect of electrode thickness variation on operation of capacitive deionization," *Electrochimica,* p. 2012, Acta.

[35] R. Zhao and O. Satpradit, "Optimization of salt adsorption rate in membrane capacitive deionization," *Water Research,* pp. 1941-1952, 2013.

[36] T. Kim and J. Yoon, "CDI ragone plot as a functional tool to evaluate desalination performance in capacitive deionization," *RSC Advances,* pp. 1456-1461, 2015.

[37] Y. Qu and P. Campbell, "Energy consumption analysis of constant voltage and constant current operations in capacitive deionization," *Desalination,* pp. 18-24, 2016.

[38] D. Oyarzun and A. Hemmatifar, "Adsorption and capacitive regeneration of nitrate using inverted capacitive deionization with surfactant functionalized carbon electrodes," *Separation and Purification Technology,* pp. 410-415, 2018.

[39] X. Shang and R. Cusick, "A combined modeling and experimental study assessing the impact of fluid pulsation on charge and energy efficiency in capacitive deionization," *Journal of the Electrochemical Society,* pp. E536-E547, 2017.

[40] M. Suss and S. Porada, "Water desalination via capacitive deionization: what is it and what can we expect from it?," *Energy and Environmental Science,* pp. 2296-2319, 2015.

[41] S. Hawks and A. Ramachandran, "Performance metrics for the objective assessment of capacitive deionization systems," *Water Research,* pp. 126-137, 2019.

[42] A. E, N. M and I. C, The Dependence of the Desalination Performance in Capacitive Deionization Processes on the Electrodes PZC, Rama-Gan: The Electrochemical Society, 2011.

47

[43] S. P. A. V. d. W. P. B. J.E. Dystra, "Energy consumption in capacitive deionization – Constant current versus constant voltage operation," *Water Research,* pp. 367-375, 2018.

[44] J. Lee and S. Kim, "Rocking Chair Desalination Battery Based on Prussian Blue Electrodes," *ACS Omega,* pp. 1653-1659, 2017.

[45] A. Johnson and A. Venolia, US Department of the Interior, Washington, 1970.

[46] A. S. E. Guyes, "A one-dimensional model for water desalination by flow-through electrode capacitive deionization," *Desalination,* pp. 8 - 13, 2017.

[47] E. Remillard, A. Shocron and J. Rahill, "A direct comparison of flow-by and flow-through capacitive deionization," *Desalination,* pp. 169-177, 2018.

[48] S. Jeon and H. Park, "Desalination via a new membrane capacitive deionization process utilizing flow-electrodes," *Energy & Environmental Science,* pp. 1471-1475, 2013.

[49] S. Jeon, J. Yeo and S. Yang, "Ion storage and energy recovery of a flow-electrode capacitive deionization process," *Journal of Materials Chemistry,* pp. 6378-6383, 2014.

[50] S. Porada, D. Weingarth and H. Hamelers, "Carbon flow electrodes for continuous operation of capacitive deionization and capacitive mixing energy generation," *Journal of Materials Chemistry,* pp. 9313-9321, 2014.

[51] A. Hemmatifar, M. Stadermann and J. Santiago, "Two-Dimensional porous electrode model for capacitive deionization," *The Journal of Physical Chemistry,* p. 24681–24694, 2015.

[52] Y. Bian, P. Liang and X. Yang, "Using activated carbon fiber separators to enhance the desalination rate of membrane capacitive deionization," *Desalination,* pp. 95-99, 2016.

[53] T. Kim, J. Dykstra and S. Porada, "Enhanced charge efficiency and reduced energy use in capacitive deionization by increasing the discharge voltage," *Journal of Colloid Interface Sciences,* pp. 317-326, 2015.

[54] X. Gao, A. Omosebi and J. Landon, "Surface charge enhanced carbon electrodes for stable and efficient capacitive deionization using inverted adsorption–desorption behavior," *Energy Environmental Sciences,* pp. 897-909, 2015.

[55] T. Kim and J. Yoon, "CDI ragone plot as a functional tool to evaluate desalination performance in capacitive deionization," *RSC Adv,* pp. 1456-1461, 2015.

[56] R. Zhao and S. Porada, "Energy consumption in membrane capacitive deionization for different water recoveries and flow rates, and comparison with reverse osmosis," *Desalination,* pp. 35-41, 2013.

[57] Y. Jande and W. Kim, "Desalination using capacitive deionization at constant current," *2013,* pp. 29-34, 2013.

[58] Y. Oren, "Capacitive Deionization (CDI) for desalination and water treatment - past, present, and future (a review)," *Desalination,* pp. 10-29, 2008.

[59] A. Hassanvand and K. Wei, "The Role of Ion Exchange Membranes in Membrane Capacitive Deionisation," *Membranes,* p. 54, 2017.

[60] P. Biesheuvel and A. Van Der Wal, "Membrane Capacitive Deionization," *Journal of Membrane Science,* pp. 256-262, 2010.

[61] H. Li and L. Zou, "Ion-exchange membrane capacitive deionization: A new strategy for brackish water desalination," *Desalination,* pp. 62-66, 2011.

[62] S. S. J. Lee, "Preparation of ion exchanger layered electrodes for advanced membrane capacitive deionization (MCDI)," *Water Research,* pp. 5375-5380, 2011.

[63] J. Lee, K. Park and S. Yoon, "Desalination performance of a carbon-based composite electrode," *Desalination,* pp. 155-161, 2009.

[64] P. Biesheuvel and A. Van Der Wal, "Energy consumption and constant current operation in membrane capacitive deionization," *Energy and Environmental Science,* pp. 9520-9527, 2012.

[65] J. Lee and S. SJ, "Preparation of ion exchanger layered electrodes for advanced membrane capacitive deionization (MCDI)," *Water Research,* pp. 5375-5380, 2011.

[66] J. Lee and S. Kim, "Hybrid capacitive deionization to enhance the desalination performance of capacitive techniques," *Energy & Environmental Science,* pp. 3683-3689 , 2014.

[67] J. Lee and K. Park, "Desalination of a thermal power plant wastewater by membrane capacitive deionization," *Desalination,* pp. 125-134, 2006.

[68] S. Jeon, H. Park and J. Yeo, "Desalination via a new membrane capacitive deionization process utilizing flow-electrodes," *Energy and Environmental Science,* pp. 1471-1475, 2013.

[69] S. Porada, D. Weingarth and V. Hamelers, "Carbon flow electrodes for continuous operation of capacitive deionization and capacitive mixing energy generation," *Journal of Material Chemistry,* pp. 9319-9321, 2014.

[70] S. Jeon and S. Yeo, "on storage and energy recovery of a flow-electrode capacitive deionization process," *Journal of Materials Chemistry A,* pp. 6378-6383, 2014.

[71] X. Gao and A. Omosebi, "Surface charge enhanced carbon electrodes for stable and efficient capacitive deionization using inverted adsorption–desorption behavior," *Energy and Environmental Science,* pp. 897-909, 2015.

[72] P. Sharma and T. Bhatti, "A review on electrochemical double-layer capacitors," *Energy Conversion and Management,* pp. 2901-2912, 2010.

[73] C. T. R. Mayes, "Mesoporous Carbon for Capacitive Deionization of Saline Water," *Environmental Science and Technology,* pp. 10243-10249, 2011.

[74] M. W. L. Wang, "Capacitive deionization of NaCl solutions using carbon nanotube sponge electrodes," *Journal of Materials Chemistry,* pp. 18295-18299 , 2011.

[75] M. G. L. X.Z. Wang, "Electrosorption of ions from aqueous solutions with carbon nanotubes and nanofibers composite film electrodes," *Applied Physics Letters,* 2006.

[76] R. Pekala, J. Farmer and C. Alviso, "Carbon aerogels for electrochemical applications," *Journal of Non-Crystalline Solids,* pp. 74-80, 1998.

[77] B. Rao, Nanostructures for Novel Therapy: Synthesis, Characterization and Applications, Elsevier, 2017.

[78] J.C. Farmer et al, "Capacitive deionization of NH4ClO4 solutions with carbon aerogel electrodes," *Journal of Applied Electrochemistry,* pp. 1007-1018, 1996.

[79] K. Yang et al, "Electrosorption of Ions from Aqueous Solutions by Carbon Aerogel: An Electrical Double-Layer Model," *Langmuir,* pp. 1961-1969, 2001.

[80] F. La Mantia, M. Pasta and H. Deshazer, "Batteries for Efficient Energy Extraction from a Water Salinity Difference," *Nano Letters,* pp. 1810-1813, 2011.

[81] M. Pasta, "A Desalination Battery," *Nano Letters,* pp. 839-843, 2012.

[82] M. Pasta, A. Battistel and F. Mantia, "Batteries for lithium recovery from brines," *Energy & Environmental Sciences,* pp. 9487-9491, 2012.

[83] J. Lee, Y. H and C. Kim, "Highly selective lithium recovery from brine using a λ-MnO2–Ag battery," *Physical Chemistry and Chemical Physics,* pp. 7690-7695, 2013.

[84] J. Lee, S. Kim and C. Kim, "Hybrid capacitive deionization to enhance the desalination performance of capacitive techniques," *Energy and Environmental Scienc,* pp. 3683-3686, 2013.

[85] H. Yoo and S. Han, ""Rocking-Chair"-Type Metal Hybrid Supercapacitors," *ACS Applied Materials and Interfaces,* pp. 30853-30862, 2016.

[86] S. Choi, B. Chang and S. Kim, "Battery Electrode Materials with Omnivalent Cation Storage for Fast and Charge-Efficient Ion Removal of Asymmetric Capacitive Deionization," *Advanced Functional Materials,* 2018.

[87] J. Lee and s. Kim, "Hybrid capacitive deionization to enhance the desalination performance of capacitive techniques," *Energy and Enironmental Sciences,* pp. 3683-3686, 2014.

[88] S. Kim and J. Lee, "Na2FeP2O7 as a novel material for hybrid capacitive deionization," *Electochim Acta,* pp. 265-271, 2016.

[89] J. Yang and L. Zou, "Preparing MnO2/PSS/CNTs composite electrodes by layer-by-layer deposition of MnO2 in the membrane capacitive deionisation," *Desalination,* pp. 108-114, 2012.

[90] H. Li and Z. Leong, "Hydrothermally synthesized graphene and Fe3O4 nanocomposites for high performance capacitive deionization," *11967-11972,* pp. 11967-11972, 2016.

[91] Y. Tsai and R. Doon, "Hierarchically ordered mesoporous carbons and silver nanoparticles as asymmetric electrodes for highly efficient capacitive deionization," *Desalination,* pp. 171-179, 2016.

[92] G. Divyapriya and K. Vijaykumar, "Development of a novel graphene/Co3O4 composite for hybrid capacitive deionization system," *Desalination,* pp. 102-110, 2019.

[93] G. Yuan and Z. Jiang, "Electrochemical behavior of activated-carbon capacitor material loaded with nickel oxide," *Carbon,* pp. 2913-2917, 2005.

[94] L. Xie, J. Wu and C. Chen, "A novel asymmetric supercapacitor with an activated carbon cathode and a reduced graphene oxide–cobalt oxide nanocomposite anode," *Jounral of Power Sources,* pp. 148-156, 2013.

[95] M. Ramani and B. Haran, "Synthesis and characterization of hydrous ruthenium oxide–carbon supercapacitors," *Journal of the Electrochemical Society,* pp. A374-A380, 2001.

[96] M. Ramani and B. Haran, "Studies on activated carbon capacitor materials loaded with different amounts of ruthenium oxide," *Journal of Power Sources,* pp. 209-214, 2001.

[97] H. SW and H. SH, "Synthesis and characterization of tin oxide/carbon aerogel composite electrodes for electrochemical supercapacitors," *Journal of Power Sources,* pp. 451-459, 2007.

[98] P. Staiti and F. Lufrani, "Investigation of polymer electrolyte hybrid supercapacitor based on manganese oxide–carbon electrodes," *Electochim Acta,* pp. 7436-7442, 2010.

[99]   D. Yang, "Pulsed laser deposition of manganese oxide thin films for supercapacitor applications," *Journal of Power Sources,* pp. 8843-8849, 2011.

[100] K. Leonard, J. Gnethe and J. Sanfilippo, "Synthesis and characterization of asymmetric electrochemical capacitive deionization materials using nanoporous silicon dioxide and magnesium doped aluminum oxide," *Electrochimica Acta,* p. 5286, 2009.

[101] L. Chu and M. Tejedor, "Particulate sol-gel route for microporous silica gels," *Microporous Materials,* p. 207, 1997.

[102] L. Zou and G. Morris, "Using activated carbon electrode in electrosorptive deionisation of brackish water," *Desalination,* pp. 329-349, 2008.

[103] M. Zafra and P. Lavela, "A novel method for metal oxide deposition on carbon aerogels with potential application in capacitive deionization of saline water," *Electrochim. Acta,* pp. 208-216, 2014.

[104] L. KC and J. Gnethe, "Synthesis and characterization of asymmetric electrochemical capacitive deionization materials using nanoporous silicon dioxide and magnesium doped aluminum oxide," *Electrochim. Acta,* pp. 5289-5291, 2009.

[105] K. Laxman and M. Myint, "Enhancement in ion adsorption rate and desalination efficiency in a capacitive deionization cell through improved electric field distribution using electrodes composed of activated carbon cloth coated with zinc oxide nanorods," *ACS Applied Materials and Interfaces,* pp. 10113-10120, 2014.

[106] M. Myint and J. Dutta, "Fabrication of zinc oxide nanorods modified activated carbon cloth electrode for desalination of brackish water using capacitive deionization approach," *Desalination,* pp. 24-30, 2012.

[107] J. Liu and M. Lu, "Capacitive desalination of ZnO/activated carbon asymmetric capacitor and mechanism analysis," *Electroochimica Acta,* pp. 312-318, 2015.

[108] T. Brousse, P. Taberna and O. Crosnier, "Long-term cycling behavior of asymmetric activated carbon/MnO2 aqueous electrochemical supercapacitor," *Journal of Power Sources,* pp. 633-641, 2007.

[109] M. Xu, D. Zhao and S. Bao, "Mesoporous amorphous MnO2 as electrode material for supercapacitor," *Journal of Solid State Electrochemistry,* pp. 1101-1107, 2007.

[110] J. Post, "Manganese oxide minerals: Crystal structures and economic and environmental significance," *Proceeding of the National Academy of Sciences of the United States of America,* pp. 3447-3454, 1999.

[111] D. C. B. Byles, "Tunnel structured manganese oxide nanowires as redox active electrodes for hybrid capacitive deionization," *Nano Energy,* pp. 476-488, 2018.

[112] F. Tedjar, "Structural modification on heat treatment of γ-MnO2," *Thermochmimica Acta,* pp. 13-22, 1991.

[113] M. Toupin, "Charge Storage Mechanism of MnO2 Electrode Used in Aqueous Electrochemical Capacitor," *Chemistry Materials,* pp. 3184-3190, 2004.

[114] A. Fischer, "Incorporation of Homogeneous, Nanoscale MnO2 within Ultraporous Carbon Structures via Self-Limiting Electroless Deposition: Implications for Electrochemical Capacitors," *Nano Letters,* pp. 281-286, 2007.

[115] M. Feng, "Manganese oxide electrode with excellent electrochemical performance for sodium ion batteries by pre-intercalation of K and Na ions," *Nature,* 2017.

[116] H. H. Y. Chen, "Manganese Oxide," April 2019. [Online]. Available: https://www.sciencedirect.com/topics/chemical-engineering/manganese-oxide.

[117] H. K. R. Chitrakar, "Recovery of lithium from seawater using managese oxide adsorbent," *Ind. Eng. Chem,* pp. 2054-2058, 2001.

[118] W. Chen and Z. Fan, "Enhanced capacitance of manganese oxide via confinement inside carbon nanotubes," *Chemical Communications,* pp. 3905-3907, 2010.

[119] A. El-Deen and N. Barakat, "Graphene wrapped MnO2-nanostructures as effective and stable electrode materials for capacitive deionization desalination technology," *Desalination,* pp. 289-298, 2014.

[120] G. Li and Z. Feng, "Mesoporous MnO2/Carbon aerogel composites as promising electrode materials for high-performance supercapacitors," *Langmuir,* pp. 2209-2213, 2010.

[121] H. Xia and M. Lai, "Nanoflaky MnO2/carbon nanotube nanocomposites as anode materials for lithium-ion batteries," *Journal of Materials and Chemistry,* pp. 6896-6902, 2010.

[122] A. Fischer and M. Saunders, "Electroless Deposition of Nanoscale MnO2 on Ultraporous Carbon Nanoarchitectures: Correlation of Evolving Pore-Solid Structure and Electrochemical Performance," *Journal of the Electrochemical Society,* 2007.

[123] S. Seo and H. Jeon, "Investigation on removal of hardness ions by capacitive deionization (CDI) for water softening applications," *Water Research,* pp. 2267-2275, 2010.

[124] K. Zuo, J. Kim and A. Jain, "Novel Composite Electrodes for Selective Removal of Sulfate by the Capacitive Deionization Process," *Environmental Science and Technology,* pp. 9486-9494, 2018.

53

[125] A. Meena and G. Mishra, "Removal of heavy metal ions from aqueous solutions using carbon aerogel as an adsorbent," *Journal of Hazardous Materials,* pp. 161-170, 2005.

[126] M. Pasta and A. Battistel, "Batteries for lithium recovery from brines," *Energy of Environmental Science,* pp. 9487-9491, 2012.

[127] S. Kim, J. Lee and J. Kang, "Lithium recovery from brine using a λ-MnO2/activated carbon hybrid supercapacitor system," *Chemosphere,* pp. 50-56, 2015.

[128] H. Y. D. S. S. Kim, "Electrochemical selective ion separation in capacitive deionization with sodium manganese oxide," *Journal of Colloid and Interface Science,* pp. 644-648, 2017.

[129] M. Bryjak, A. Siekierka and J. Kujawski, "Capacitive Deionization for Selective Extraction of Lithium from Aqueous Solutions," *Journal of Membrane and Separation Technology,* pp. 110-115, 2015.

[130] P. Srimuk, "Potential-Dependent, Switchable Ion Selectivity in Aqueous Media Using Titanium Disulfide," *ChemSusChem,* 2018.

[131] A. Hassanvand and G. Chen, "A comparison of multicomponent electrosorption in capacitive deionization and membrane capacitive deionization," *Water Research,* pp. 100-109, 2018.

[132] C. Hou and C. Huang, "A comparative study of electrosorption selectivity of ions by activated carbon electrodes in capacitive deionization," *Desalination,* pp. 124-129, 2013.

[133] T. H. C. Di Maio, Chemo-Mechanical Coupling in Clays: From Nano-scale to Engineering Applications, CRC Press, 2002.

[134] A. T. Conlisk, Essentials of Micro- and Nanofluidics: With Applications to the Biological and Chemical Sciences, Cambridge university Press, 2013.

[135] T. G.Canham, Descriptive Inorganic Chemistry, Third Edition, Macmillan, 2003.

[136] L. B. Railsback, "Some Fundamentals of Mineralogy and Geochemistry," 2006. [Online]. Available: www.gly.uga.edu/railsback/FundamentalsIndex.html.

[137] K. P. A. Fischer, "Incorporation of Homogeneous Nanoscale MnO2 within Ultraporous Carbon Structures vie Self Limiting Electroless Deposition: Implications for Electrochemical Capacitors," *American Chemical Society,* pp. 282-286, 2006.

[138] M. Sassin et al, "Achieving electrochemical capacitor functionality from nanoscale LiMn2O4 coatings on 3-D carbon nanoarchitectures," *Journal of Materials Chemistry,* 2013.

[139] M. Donakowski et al, "Crystal Engineering in 3D: Converting nanoscale lamellar manganese oxide to cobic spinel while affixed to a carbon architectur," *CrystEngComm,* pp. 6035-6048, 2016.

[140] Y. Lui and C. Nie, "Review on carbon-based composite materials for capacitive deionizatio," *RSC Advances,* pp. 15205-15225, 2014.

[141] X. Zhang and T. Chen, "MgFe2O4/reduced graphene oxide composites as high-performance anode materials for sodium ion batteries," *Electrochimica Acta,* pp. 616-621, 2015.

[142] J. A. Trainham, "A Flow-Through Porous Electrode Model: Application to Metal-Ion Removal from Dilute Streams," *Journal of the Electrochemical Society,* pp. 1528-1540, 1977.

[143] D. F. G. M. R. P. J.C. Farmer, "Capacitive, deionization with carbon aerogel electrodes: Carbonate, sulfate, and phosphate," *The Journal of the Electrochemical Society,* p. 14, 1995.

[144] L. K. H. Ali. R. Ashwin, "Thermodynamics of Ion Separation by Electrosorption".

[145] D. Reible, Fundamentals of Environmental Engineering, CRC Press, 2017.

[146] T. K. J. Kang, "Comparison of salt adsorption capacity and energy consumption between constant current and constant voltage operation in capacitive deionization," *Desalination,* pp. 52-57, 2014.

[147] P. Q. Ashton Acton, Advances in Nanotechnology Research and Application: 2012 Edition, 14170, 2012.

[148] e. a. J. Lee, "Desalination of a thermal power plant wastewater by membrane capacitive deionization," *Desalination,* pp. 125-134, 2006.

[149] A. Eftekhari and D.-W. Kim, "Sodium Ion Batteries: New opportunities beyound energy storage in lithium," *Journal of Power Source,* pp. 336-348, 2018.

[150] J. G. J. Song, "Sodium manganese oxide electrodes accompanying self-ion exchange for lithium/sodium hybrid ion batteries," *Electrochimica Acta,* pp. 42-48, 2018.

[151] U. o. Birmingham, "New high-capacity sodium-ion could replace lithium in rechargeable batteries," 13 April 2019. [Online]. Available: www.sciencedaily.com/releases/2018/09/180912111913.htm.

[152] K. B.S.Singu, "Exfoliated graphene-manganese oxide nanocomposite electdoe materials for supercapacitor," *Journal of Alloys and Compounds,* pp. 1189-1199, 2019.

[153] S. Z. H. Yin, "Three-Dimensional Graphene/Metal Oxide Nanoparticle Hybrids for High-Performance Capacitive Deionization of Saline Water," *Advanced Materials,* pp. 6270-6276, 2013.

[154] G. W. T. Wu, "Highly Stable Hybrid Capacitive Deionization with a MnO2 Anode and a Positively Charged Cathode," *Environmental Science and Technology,* pp. 98-102, 2018.

[155] J. L. H. Yoon, "Hybrid capacitive deionization with Ag coated carbon composite electrode," *Desalination,* pp. 42-48, 2017.

[156] M. Gaikwad, "Capacitive Deionization for Desalination Using Nanostructured Electrodes," *Analytical Letters,* pp. 1641-1655, 2016.

[157] J. Barrett, Inorganic Chemistry in Aqueous Solution, Royal Society of Chemistry, 2003, p. 184.

[158] Y.Marcus, "Thermodynamics of Solvation of Ions," *Journal of the Chemical Society,* pp. 2995-2999, 1991.

[159] P. Biesheuvel and J. Dystra, "The difference between Faradaic and Nonfaradaic processes in Electrochemistry," 2018.

[160] M. Suss and V. Presser, "Water Desalination with Energy Storage Electrode Materials," *Joule 2,* pp. 10-15, 2018.

[161] R. Liu and J. Duay, "Redox Exchange induced MnO2 nanoparticle enrichment in poly(3,4-ethylenedioxythiophene) nanowires for electrochemical energy storage," *ACS Nano,* pp. 4299-4307, 2010.

[162] S. Postel, Last Oasis: Facing Water Scarcity, New York: W.W. Norton & Company, 1992.

[163] J. Lee and C. Lee, "Desalination of a thermal power plant wastewater by membrane capacitive deionization," *Desalination,* pp. 125-134, 2006.

[164] M. Sassin and A. Mansour, "Electroless Deposition of Conformal Nanoscale Iron Oxide on Carbon Nanoarchitectures for Electrochemical Charge Storage," *ACS Nano,* pp. 4505-4514, 2010.

[165] L. Aravinda, U. Bhat and R. Bhat, "Nano CeO2/activated carbon based composite electrodes for high performance supercapacitor," *Materials Letters,* 2013.

[166] P. Simon, Electrochemical Capacitors and Hybrid Power Batteries 2008, Issue 1, The Electrochemical Society, 2008.

[167] "Electrochemical Capacitors," 09 May 2019. [Online]. Available: http://energystorage.org/energy-storage/technologies/electrochemical-capacitors.

[168] "Introduction to Electrochemical Capacitor Technology," *IEEE Electrical Insulation Magazine,* pp. 40-47, 09 May 2019.

[169] B. Conway, Electrochemical Supercapacitors: Scientific Fundamentals and Technological Applications, Springer Science & Business Media, 2013.

[170] A. Yu and V. Chabot, Electrochemical Supercapacitors for Energy Storage and Delivery: Fundamentals and Applications, CRC Press, 2017.

[171] X. Tang and Z. Qi, "Economic analysis of EDLC/battery hybrid energy storage," in *2008 International Conference on Electrical Machines and Systems*, 2019.

[172] B. Xu, F. Wu and R. Chen, "Highly mesoporous and high surface area carbon: A high capacitance electrode material for EDLCs with various electrolytes," *Electrochemistry Communications,* pp. 795-797, 2008.

[173] F. Xing, T. Li and J. Li, "Chemically exfoliated MoS2 for capacitive deionization of saline water," *Nano Energy,* pp. 590-595, 2017.

[174] J. Wouters, J. Lado and M. Anderson, "Low Surface Area Carbon Fiber Electrodes Coated with Nanoporous Thin-Films of γ–Al2O3 and SiO2: Relationship between Coating Conditions, Microstructure and Double Layer Capacitance," *Journal of the Electrochemical Society,* pp. A1374-A1382, 2012.

[175] K. Laxman, M. Myint and H. Bourdoucent, "Enhancement in Ion Adsorption Rate and Desalination Efficiency in a Capacitive Deionization Cell through Improved Electric Field Distribution Using Electrodes Composed of Activated Carbon Cloth Coated with Zinc Oxide Nanorods," *ACS Applied Materials Interfaces,* p. 10113–10120, 2014.

[176] M. Zafra and P. Lavela, "A novel method for metal oxide deposition on carbon aerogels with potential application in capacitive deionization of saline water," *Electrochimica Acta,* pp. 208-216, 2014.

[177] T. Kim, J. Dystra and S. Porada, "Enhanced charge efficiency and reduced energy use in capacitive deionization by increasing the discharge voltage," *J. Colloid Interface Sci,* pp. 317-326, 2015.

[178] G. Murphy and D. Caudle, "Mathematical theory of electrochemical demineralization in flowing systems," *Electrochim Acta,* pp. 1655-1664, 1967.

[179] G. Murphy, J. Cooper and J. Hunter, "Activated carbon used as electrodes in electrochemical demineralization of saline water," *U.S. Dept. of the Interior,* 1969.

[180] Y. Oren and A. Soffer, "Electrochemical parametric pumping," *Journal of Electrochemical Society,* pp. 869-875, 1978.

[181] A. Soffer and M. Folman, "The electrical double layer of high surface porous carbon electrode," *J Electroanalyctic Chem Interfacial Electrochem,* pp. 25-43, 1972.

[182] Y. Oren and A. Soffer, "Water desalting by means of electrochemical parametric pumping. II. Separation properties of a multistage column," *Journal of Applied Electrochemistry,* pp. 489-505, 1983.

[183] J. Farmer, "The use of capacitive deionization with carbon aerogel electrodes to remove inorganic contaminants from water," U.S. Department of Energy Office of Scientific and Technical Information, Orlando, 1995.

[184] X. Gao and A. Ososebi, "Enhanced Salt Removal in an Inverted Capacitive Deionization Cell Using Amine Modified Microporous Carbon Cathodes," *Environmental Science and Technology,* pp. 10920 - 10926, 2015.

[185] Super Course in Chemistry for the IIT JEE: Physical Chemistry, Pearson Education India.

[186] E. Stansbury and R. Buchanan, Fundamentals of Electrochemical Corrosion, ASM International, 2000.

[187] N. Kularatna, Energy Storage Devices for Electronic Systems: Rechargeable Batteries and Supercapacitors, Academic Press, 2014.

[188] W. Tang, J. Liang and D. He, "Various cell architectures of capacitive deionization: Recent advances and future trends," *Water Research,* pp. 225-251, 2019.

[189] S. Yang, J. Choi and J. Yeo.

[190] R. Meade, "Foundations of Electronics," 2002.

Figure 15: Questions 1 and 2: Where do we get our water from? Who regulates its quality?

	BSA		FSA	
	Question 1	Question 2	Question 1	Question 2
Pre Quiz	72%	29%	18%	45%
Post Quiz	100%	71%	-	-

Figure 16: Question 3: Can you see yourself studying engineering/science?

	BSA		FSA
	Pre Quiz	Post Quiz	Pre Quiz
Yes	41%	48%	36%
No	38%	45%	9%
Maybe/IDK	22%	6%	55%

Additional responses to pre and post quiz:

From Betty Shabazz International Charter School students

PRE: "Yes, because I attend various engineering events, I also attend a program at Chicago State University every Saturday and we will be attending NSBE in March."

PRE: "Yes, because I like studying the earth and tech."

POST: "I think possibly because my dad is an engineer"

No:

PRE: "No, I cannot because science isn't something that I would enjoy for a career"

PRE: "No, because I will admit I'm not that smart - a hard no"

POST: "I don't because nothing in science/engineering has been interesting to me"

POST: "No, because I'm more of a business person"

POST: "No, because it looks like a lot of work"

Maybe/Probably:

PRE: "Not right now. It is too complex for me but when I school (3 or 4 years), I will probably study in to that and architectural things at Lindbloom [a high school in Chicago].

POST: "Probably because I learned a lot today"

From Franklin Middle School students

PRE: "Maybe, but I won't pursue it as a career. Maybe as a hobby though."

PRE: "No."

PRE: "Yes, I love engineering!"

PRE: "Maybe, but I honestly want to go to the Olympics."

PRE: "Yes, I am SMART."

Figure 17: The children from the Chicago location and myself assembling a sand filter.

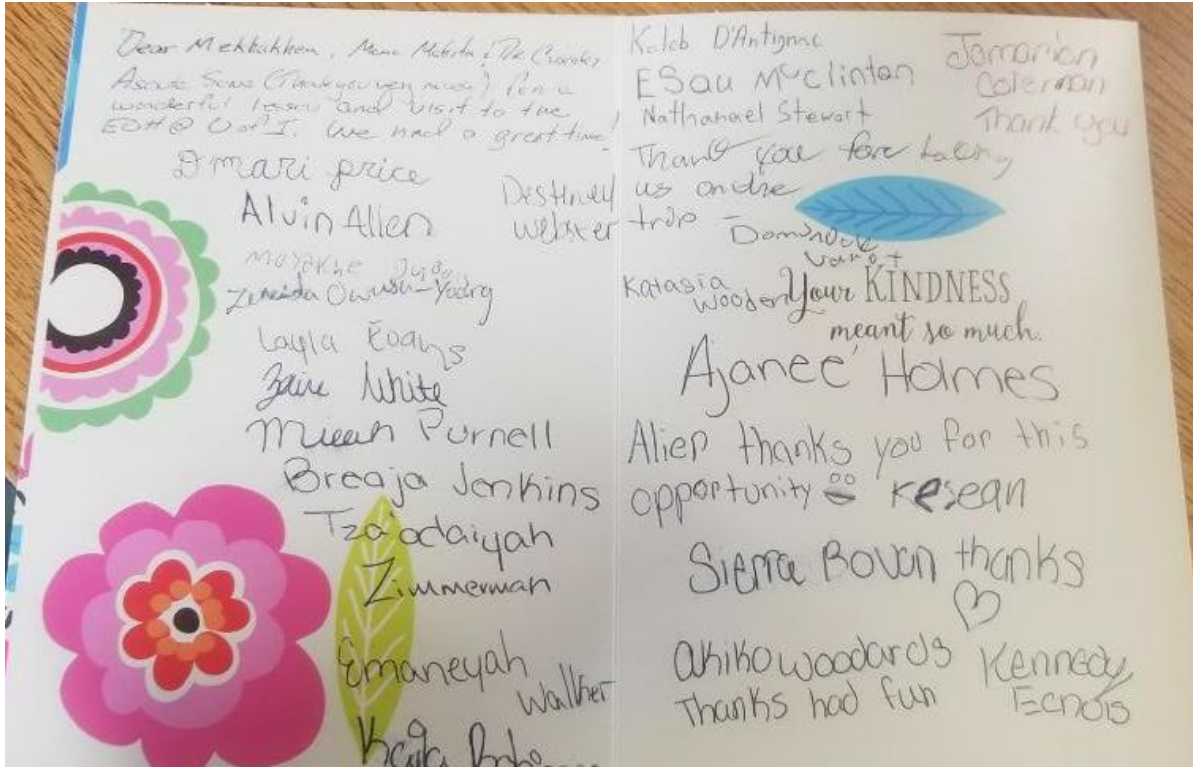Figure 18: Dr. Roland Cusick and a group of children from the Chicago location during the demonstration.

Figure 19: A Thank You card sent from the student at the Chicago location.